Foam as a Vehicle for Nanoparticle Delivery in Unsaturated Porous Media

by

Zahra Sadeghi Ardestani

A thesis
presented to the University of Waterloo
in fulfillment of the
thesis requirement for the degree of
Master of Applied Science
in
Civil Engineering

Waterloo, Ontario, Canada, 2019

AUTHOR'S DECLARATION

I hereby declare that I am the sole author of this thesis. This is a true copy of the thesis, including any required final revisions, as accepted by my examiners. I understand that my thesis may be made electronically available to the public.

Abstract

For the treatment of contaminated sites, liquid-based delivery of engineered nanoparticles (ENPs) to the unsaturated zone is a challenge due to the limited lateral transport and restricted contact between ENPs and contaminants. Foam is potentially capable of overcoming some of the challenges associated with liquid-based delivery of ENPs. The capability of foam to deliver Pluronic coated iron oxide core nanoparticles in unsaturated porous media was investigated. A multi-criteria decision analysis (MCDA) was used to select preferred surfactants which were then screened to determine foam properties, and used in a column transport study to investigate the capability of foam to transport ENPs in unsaturated media.

Based on the MCDA results, Steol CS-460, Bioterge AS-40, SDS, Ammonyx LO, and Rhamnolipids were selected. These surfactants were added to Milli-Q water or synthetic groundwater to prepare foaming solutions, and the properties (i.e., foamability and foam stability) of the generated foams were determined. Steol CS-460 and Bioterge AS-40 were shown to have the highest foamability and foam stability and therefore, were selected for the subsequent experimental efforts. Ammonyx LO was also used for comparison purposes. The three surfactants enhanced the foamabilitiy of the ENPs. Steol CS-460 and Bioterge AS-40 increased the foam stability of the ENPs, whereas Ammonyx LO did not noticeably change it. Foams generated by Steol CS-460, Bioterge AS-40, or Ammonyx LO were able to support the ENPs. It was demonstrated that for foam generation, the ENPs were compatible with the foamability of the surfactants and the foam stability of Bioterge AS-40, and Ammonyx LO. However, the stability of the foam generated by Steol CS-460 slightly decreased from 99.2% ± 0.9% to 90.5% ± 0.7% in the presence of the ENPs.

The column experiments were designed and conducted to evaluate the capability of foam generated by Steol CS-460, Bioterge AS-40, and Ammonyx LO to transport the ENPs in unsaturated media. The impact of surfactant type and concentration, and initial volumetric water content of the unsaturated porous medium on the capability of foam to transport the ENPs were investigated. A total of five trials were conducted; four in initially partially saturated media, and one in an initially dry medium. The surfactant type was found to affect the capability of foam to transport the ENPs as the ENP mass recovery by the Steol CS-460 foam (101%) and Bioterge AS-40 foam (93%) were significantly higher than the ENP mass recovery by the Ammonyx LO foam (54%), and the ratio of foam outflow rate to the average foam inflow rate was the lowest for Ammonyx LO. The ENP mass recovery remained essentially unchanged as the Steol CS-460 concentration decreased from 0.3 to 0.1 wt%. Furthermore,

as the initial volumetric water content of the porous medium decreased from 0.2 to dry condition, the ENP and tracer mass recoveries by the Steol CS-460 foam slightly decreased.

Overall, the results of the column experiments indicate that the foam generated by Steol CS-460 at a concentration of 0.3 and 0.1 wt% was successfully capable to deliver Pluronic coated iron oxide core nanoparticles in unsaturated porous media, and thus foam has the potential to deliver the ENPs *in situ*. The column experiments are the first trials in which the capability of foam generated from various surfactants to deliver the ENPs in unsaturated media was investigated, and an attempt was made to completely recover the delivered ENPs.

Acknowledgements

First, I would like to express my gratitude to my supervisor, Dr. Neil R. Thomson, for his guidance and support through the completion of this research. Second, I am grateful to all technicians who provided guidance in the lab work of this research: Terry Ridgway, Mark Merlau, Mark Sobon, Shirley Chatten, and Ralph Dickhout. Finally, thank you to my friends and colleagues in Groundwater and Soil Remediation Lab that helped me de-stress and enjoy the research process.

This research was financially supported by a Natural Sciences and Engineering Research Council (NSERC) of Canada Collaborative Research and Development Grant (N.R. Thomson), as well as Chevron Energy Technology Company.

Dedication

I would like to dedicate this thesis to my parents, Shahnaz and Yaghoub, whose words of encouragement kept me going throughout the research process. My brothers, Mohsen and Amir, were always there for me and are very special.

Table of Contents

List of Figures

List of Tables

Chapter 1
Introduction

Accidental releases, spills, and leaks of petroleum hydrocarbons (PHCs), such as gasoline and jet fuel, can result in subsurface contamination. PHCs that become entrapped as a residual light non-aqueous phase liquid (LNAPL) in the unsaturated zone often serve as a long-term source to groundwater contamination depending on the composition (USEPA 2012; Lee et al. 2001). Technologies used to remediate these residuals are categorized according to where the treatment occurs (*in situ* vs *ex situ*). *In situ* treatment technologies are preferred by the remediation community since they are typically more economical, efficient, and environmentally friendly (Agarwal and Liu 2015; Kuppusamy et al. 2016; Song et al. 2017).

Nanoremediation is an emerging *in situ* treatment technology that has received attention since it has the potential to reduce both the cost and the time to clean-up contaminated sites (Tratnyek and Johnson 2006; Kuppusamy et al. 2016). Nanoremediation obtains its advantage from the use of nanoparticles (NPs) that have higher reactivity owing to their increased surface area (Theron et al. 2008). The most widely used NPs in groundwater remediation is nano-scale zero-valent iron (nZVI) (Crane and Scott 2012). Successful delivery of NPs as well as sufficient contact between NPs and the contaminant is needed for effective treatment (Schrick et al. 2004; Zhao et al. 2016). NPs have been engineered to enhance their mobility in porous media so that they can travel further into contaminated zones and hence, improve overall treatment efficiency (Karn et al. 2009). The mobility of NPs is dependent on a wide range of factors such as the physicochemical properties of NPs (e.g., size, surface properties, and surface charge) and porous medium (e.g., type, surface properties, and grain size) (Wang et al. 2016). For a given NP within an unsaturated porous medium, mechanisms such as attachment to grains and immobile air-water interfaces govern NP mobility (DeNovio et al. 2004). Recently, Linley et al. (2019) developed novel NPs (Pluronic coated with an iron oxide core) that are highly mobile and have the ability to bind to LNAPLs (e.g., crude oil).

Appropriate delivery of these engineered nanoparticles (ENPs) into the unsaturated zone is crucial for effective treatment. ENPs are typically delivered into the unsaturated zone as a solution that is gravity-fed or injected under pressure (i.e., liquid-based delivery). This delivery method in the unsaturated zone is associated with a number of challenges limiting ENP application. First, liquids tend to migrate downward due to gravity, which subsequently results in limited lateral ENP transport and thereby restricts the radius of influence. Second, liquids generally prefer to migrate through zones with

higher permeability and bypass lower-permeability zones. As a consequence, contact between the ENPs and contaminants in lower-permeability zones may be restricted, leading to limited treatment. (Shen et al. 2011; Su et al. 2014). Given the importance of ENP delivery for successful *in situ* treatment and taking into account concerns regarding liquid-based delivery, there is a need to improve the delivery of ENPs in the unsaturated zone.

Liquid foam or foam is potentially capable of overcoming the intrinsic challenges associated with liquid-based delivery of ENPs in the unsaturated zone. Foam is a particular kind of colloidal dispersion in which a gas is dispersed in a continuous liquid phase. In contrast to liquid, foam is not dominated by gravity in porous media, and therefore can increase the lateral transport of ENPs (Shen et al. 2011). In addition, foam has the capability to overcome physical heterogeneities thereby giving rise to a nearly uniform flow in these regions (Bertin et al. 1998; Kovscek and Bertin 2003). Foams can be generated from polymers (e.g., proteins, polysaccharides, and hydroxypropyl methyl celluloses), synthetic surfactants (e.g., sodium dodecyl sulfate and sodium lauryl ether sulfate), or biosurfactants (e.g., rhamnolipids) (da Rosa et al. 2015; Shen et al. 2011; Hegge et al. 2010; Reddy et al. 1999; Dickinson & Izgi 1996; Richert et al. 1974; Lees & Jackson 1973).

Foam stability and foamability are two important properties used to characterize foam. The former refers to the ability of foam to resist bubble breakdown and is dependent on the foaming agent, concentration, and type of porous medium (Zhang et al. 2009), while the latter represents the ability of a foaming agent to generate foam. The stability of foam with a known initial volume can be quantified by foam half-life (time required for half of the foam volume to collapse) (Zhong et al. 2009; Wang & Mulligan 2004b; Mulligan and Eftekhari 2003). The Ross Miles Test (ASTM, 2015) is normally used to determine foam stability and foamability.

Several studies have investigated the effect of surfactant type and concentration on foam stability (da Rosa et al. 2015; Wang and Chen 2012; Shen et al. 2011; Zhong et al. 2009; Mulligan and Wang 2006; Wang & Mulligan 2004b; Mulligan and Eftekhari 2003). Mulligan and Eftekhari (2003) assessed the stability of foam generated by ten surfactants among which Triton X-100 and JBR425 (i.e., mixed rhamnolipids) had the highest foam stability. Wang and Mulligan (2004b) and Mulligan and Wang (2006) investigated the stability of foam generated by a rhamnolipid at three concentrations (0.5, 1.0, and 1.5 wt%), and reported that foam stability increased with an increase in concentration. Zhong et al. (2009) reported no clear correlation between foam stability and surfactant concentration (Steol-CS-330 at a concentration from 0.5 to 1.5 wt%). Wang and Chen (2012) determined the stability of foam

generated by sodium dodecyl sulfate (SDS), Triton X-100, and polyethylene glycol lauryl ether (Brij35) at 0.5 wt% concentration, and reported that SDS and Triton X-100 had the highest foam stability and foam generated from Brij35 had the lowest stability. da Rosa et al. (2015) investigated the stability of foam generated by SDS, cetyltrimethylammonium bromide (CTAB), and rhamnolipids and reported that the foam stability of CTAB was lower than that of SDS, and the foam stability of rhamnolipids was dependent on concentration and pH. Shen et al. (2011) evaluated the stability of foam generated by six surfactants at 1.0 wt% and determined the order of the stability as sodium lauryl ether sulfate (SLES) > SDS > Tween-20 > AEO-9 > Tween 80 > Triton X-100.

Surfactants have been widely used to generate foam for use in soil and groundwater remediation (Jeong et al. 2000; Wang & Mulligan 2004a; Wang & Chen 2012; Longpr´e-Girard et al. 2016; Maire and Fatin-Rouge 2017). The structure of surfactant comprises of a hydrophilic head and a hydrophobic tail. Surfactants are categorized into four groups (anionic, cationic, non-ionic, and zwitterionic) depending on the charge of the hydrophilic head. Anionic and cationic surfactants bear negative and positive charges in their hydrophilic head, respectively. Zwitterionic surfactants carry both negative and positive charges, and non-ionic surfactants bear no ionic charge. Charge type and critical micelle concentration (CMC) are two important surfactant characteristics for soil and groundwater remediation. (Rosen & Kunjappu 2012; Mittal 1979). Anionic surfactants are generally expected to have less adsorption to soils compared with non-ionic and cationic surfactants due to the fact that soil surfaces are usually negatively charged (Harwell et al. 1999; Huang et al. 1997). If a substantial amount of surfactant is adsorbed onto particle surfaces, foam generation will decrease as a result of less available surfactant mass, and the soil surface may become more hydrophobic, which may increase contaminant adsorption and thereby impede remediation (Del Campo Estrada 2015). In addition, anionic surfactants generally have better foam stability than non-ionic surfactants which are poor foaming agents (Urum and Pekdemir 2004; Urum et al. 2005; Rosen and Kunjappu 2012). For a given surfactant, the CMC is a specific concentration above which the molecules of the surfactant form an aggregate. When the surfactant concentration exceeds the CMC, the aqueous solubility of non-aqueous phase liquid (NAPLs) is enhanced (Mittal 1979). Previous research has shown that a surfactant concentration above the CMC is required to provide enough foamability (Del Campo Estrada 2015).

Numerous laboratory studies have used foam generated from surfactants to investigate aspects of soil and groundwater treatment in the saturated zone. Foam has been shown to enhance NAPL removal by mobilization, solubilization, and volatilization in saturated soils in column and sandbox experiments

(Rothmel et al. 1998; Reddy et al. 1999; Mulligan and Eftekhari 2003; Maire et al. 2015; Longpr´e-Girard et al. 2016). Foam has also been reported to successfully remove heavy metals (i.e., nickel and cadmium) in saturated soil columns (Wang and Mulligan 2004b; Mulligan and Wang 2006). The first field demonstration of surfactant foam to remove a dense non-aqueous phase liquid (DNAPL) was conducted by Hirasaki et al. (1997). These authors reported that foam reduced the DNAPL saturation by ~90 % in a heterogeneous alluvial aquifer. While these studies provided valuable insight into some aspects of foam technology, they evaluated foam in the saturated zone only, and did not use foam to aid reagent delivery. Appendix A provides an overview of foam generation methods, and additional details from other studies that used foam for remediation of the saturated zone.

There are only a few laboratory studies that have used foam to deliver reagents into contaminated unsaturated porous media. Zhong et al. (2009) used foam generated from SLES to deliver calcium polysulfide (CPS) to an unsaturated porous medium contaminated by chromium(VI). The authors reported a decrease in mobilized chromium(VI) from over 75 % to < 10 %. In another study, Zhong et al. (2011) concluded that delivering CPS by foam generated from SLES to an unsaturated porous medium contaminated by technetium increased stabilization of technetium from < 10 % to > 65 %. Srirattana et al. (2017) used SLES foam to deliver nZVI into an unsaturated porous medium contaminated by trichloroethylene (TCE). This was followed by the application of a low frequency-electromagnetic field (LF-EMF) to induce the nZVI NPs to generate heat and subsequently enhance TCE volatilization. The authors reported that TCE volatilization in the presence of the LF-EMF was more than 39 times higher than without the application of the LF-EMF.

To the best of our knowledge, there exist only a few studies that have used foam as a vehicle for ENP delivery in the unsaturated zone. Ding et al. (2013) investigated the transport of nZVI by SLES foam in unsaturated sand-packed columns. Su et al. (2015) assessed the use of both SDS foam and solution as vehicles to deliver nZVI in unsaturated soil columns. In these studies, the authors reported nZVI recovery (defined as the fraction of the total injected nZVI mass observed in column effluent) to investigate the feasibility of surfactant foam or solution for nZVI delivery. Although these efforts provide effective insight for ENP delivery by foam, the authors did not attempt to completely remove the injected nZVI from the columns.

Further research is needed to explore foam as a vehicle for ENP delivery in the unsaturated zone. In this research, we seek to investigate the potential for using foam generated from surfactants as a vehicle to transport Pluronic coated iron oxide core NPs in unsaturated media. To this end, the compatibility of

the ENPs on foamability and foam stability of the surfactants, and the capability of foam to deliver the ENPs in unsaturated media are investigated.

1.1 Thesis Objectives

The objectives of this research are: (1) to assess the compatibility of Pluronic coated iron oxide core NPs on the foamability and stability of foam generated from various surfactants, and (2) to investigate the capability of foam to deliver Pluronic coated iron oxide core NPs in unsaturated media.

1.2 Thesis Organization

Chapter 2 describes the materials and methods used. Chapter 3 presents an evaluation of suitable foaming agents and discusses results from a series of column experiments. Finally, Chapter 4 summarizes the conclusions of this research, and provides recommendations for future work.

Chapter 2
Methodology

2.1 Multi-Criteria Decision Analysis

Multi-criteria decision analysis (MCDA) was performed on the most frequently used foaming agents reported in the literature for soil and groundwater remediation (Table 2.1). The goal of this analysis was to select the most suitable foaming agents to use in experimental efforts. The MCDA method was used to evaluate i foaming agents by assessing them against a set of j criteria. Each criterion was assigned a weight such that it reflected the importance of that criterion. The foaming agents were scored for each criterion using a scoring scale extending from 0 to 100. The score of 0 and 100 were assigned to the least- and most-preferred foaming agents with regard to the criterion, respectively. Scores were assigned to the remaining foaming agents such that differences in the scores represented differences in strength of preference. The overall score for each agent, S_i, is as follows (Dodgson et al. 2009):

$$S_i = w_1 s_{i1} + w_2 s_{i2} + w_3 s_{i3} + \cdots + w_j s_{ij} = \sum_{j=1}^{n} w_j s_{ij} \quad (1)$$

w_j is the weight for jth criterion, s_{ij} is the score of ith foaming agent for the jth criterion, and n is the total number of the criteria. To assess the impact of criterion weight uncertainty on the selected foaming agents, different sets of weights were assigned to the criteria, and in each set of weights, the weight associated with each criterion was swung from the upper weight value to the lower weight value, here referred to as swing weight assessment. Then, the difference in the overall scores of the foaming agents were investigated. Finally, the foaming agents with the lowest scores were eliminated, and the remaining were selected for use in screening tests.

Table 2.1. Properties of selected foaming agents.

Surfactant	Origin of synthesis	Health Hazard	Biodegradability	Charge Type	CMC @ 25 °C (g/L)	Cost (CAD dollar/~1 kg)[i]
Sodium Dodecyl Sulfate (SDS)	Synthetic	Moderate Hazard[a]	Readily biodegradable[a]	Anionic	2.3[f]	40
STEOL CS-460 (SLES)	Synthetic	Slight Hazard[b]	Readily biodegradable[c]	Anionic	0.074[c]	~7
Bioterge AS-40	Synthetic	Severe Hazard[b]	Readily biodegradable[c]	Anionic	0.301[c]	~8
Triton X-100	Synthetic	Moderate Hazard[a]	Not readily biodegradable[a]	Non-ionic	0.15[d]	~29
Rhamnolipids	Biosurfactant	Minimal Hazard[a]	Readily biodegradable[d]	Anionic	0.03[g]	~1902
Ammonyx LO	Synthetic	Moderate Hazard[c]	Readily biodegradable[c]	Zwitterionic	0.011[c]	~7
Dihexylsulfosuccinate (DHSS)	Synthetic	Slight Hazard[a]	Not readily biodegradable[e]	Anionic	15[h]	~66

[a] Sigma-Aldrich Co. (2016&2015)
[b] Adapted from Stepan Co. (2016&2015)
[c] Stepan Co. (2017, 2016, 2014, 2013, 2012)
[d] Adapted from Mulligan & Eftekhari (2003)
[e] Cytec Inc. 2013
[f] Couto et al. (2009)
[g] Adapted from Mulligan et al. (2001)
[h] Adapted from Maire & Fatin-Rouge (2017)
[i] from 2017

2.2 Materials

Steol CS-460, Bioterge As-40, and Ammonyx LO were obtained from the Stepan company (Northfield, IL, USA). Rhamnolipids and Sodium Dodecyl Sulfate (SDS) were obtained from the Sigma-Aldrich company (St. Louis, MO, USA). The ENPs used in this research are neutrally charged and comprise of an iron core (SPIONs: Fe_3O_4, Fe_2O_3) with an amphiphilic polymer coating (Pluronic P104) which is a surfactant (Linley et al. 2019). The synthesis method of the ENPs was reproduced from Linley et al. (2019). Briefly, $FeSO_4 \cdot 7H_2O$ and $FeCl_3 \cdot 6H_2O$ were added to deoxygenated water at a molar ratio of 2:3 ($FeSO_4$:$FeCl_3$). Sufficient NH_4OH and oleic acid were added to achieve final concentrations of 4 and 0.22 mol/L, respectively. This solution was stirred at 70 °C for 1 h, then stirred at 90 °C under flowing N_2 for 1 h to purge evolved NH_3 gas. After cooling to room temperature, the black, magnetic precipitate was recovered by magnetic decantation and washed 3x by deoxygenated Millipore DI water (Millipore Elix 5), and then 3x by ethanol before being dried under flowing N_2. The Borden material (d_{10} = 0.075 mm) that primarily comprise of sand (>99%) with negative surface charge

was collected from the University of Waterloo Groundwater Research Facility at the Canadian Forces Base (CFB) in Borden, ON, Canada.

2.3 Screening Tests

The Ross Miles Test (ASTM, 2015) was employed to determine the effect of surfactant type and concentration on the foamability and foam stability of each surfactant. The apparatus, purchased from VWR International Co. (Radnor, PA, USA), consists of a glass foam receiver and a 200 mL glass foam pipet. An image of the apparatus is provided in Appendix B. The foamability of a surfactant was determined by its initial foam height (h_0) in the apparatus, and the foam stability was defined as the ratio of the foam height after 5 minutes to the initial foam height. The initial foam height was typically the largest height reached; however, for some of the tests, the initial foam height (h_0) increased over time and attained a height that was greater than the initial height ($h_0^* > h_0$), before the foam started to collapse. In this case, modifications were applied to the method such that the readings were taken for 5 minutes after h_0^* was reached, and foam stability was defined as the ratio of the last reading to h_0^*.

A surfactant concentration range (0.01, 0.05, 0.1, 0.3, 0.5, 1, and 1.5 wt%) was selected so that it included concentrations above the CMC (Table 2.1) for each surfactant. Each surfactant was added to Milli-Q water (MQW) or synthetic groundwater (SGW) to prepare the foaming solution. SGW was prepared following Middeldorp et al. (1998) with a slight modification to reduce the concentration of calcium and sulfate (1.0 mM $CaCl_2$ and 0.06 mM Na_2SO_4). Each foaming solution was used to generate foam in the test apparatus and hence, determine the foamability and foam stability of the surfactant. To assess the effect of SGW on the foamability and foam stability, foaming solutions prepared by MQW were compared to those prepared by the SGW. Based on the results of these tests, surfactants were selected for the subsequent experimental efforts considering those that had the highest foamability and foam stability using both MQW and SGW.

2.4 Foam Generation

An experimental set-up was built to generate foam at the bench-scale for use in column experiments (Figure 2.1). The foam generation column (FG column) was made of transparent acrylic with a 2.5 cm inner diameter and length of 30 cm. A circular porous stone (~0.64 cm thick, 2.5 cm diameter) (Humboldt Mfg. Co.) was installed at the bottom and enabled foam generation in the presence of a foaming solution and air. The foaming solution was stirred on a magnetic stirrer (IKA C-MAG HS 7) for approximately five minutes to ensure a homogeneous solution. A Masterflex L/S peristaltic pump

(Cole Parmer, 7535-08) was used to inject the foaming solution into the FG column at a rate of 1 mL/min so that a layer of the solution was formed on the porous stone. Ambient air was then introduced (40 mL/min) into the column to enable foam generation. To control air flow, a mass flow controller (OMEGA, FMA5512A) was employed.

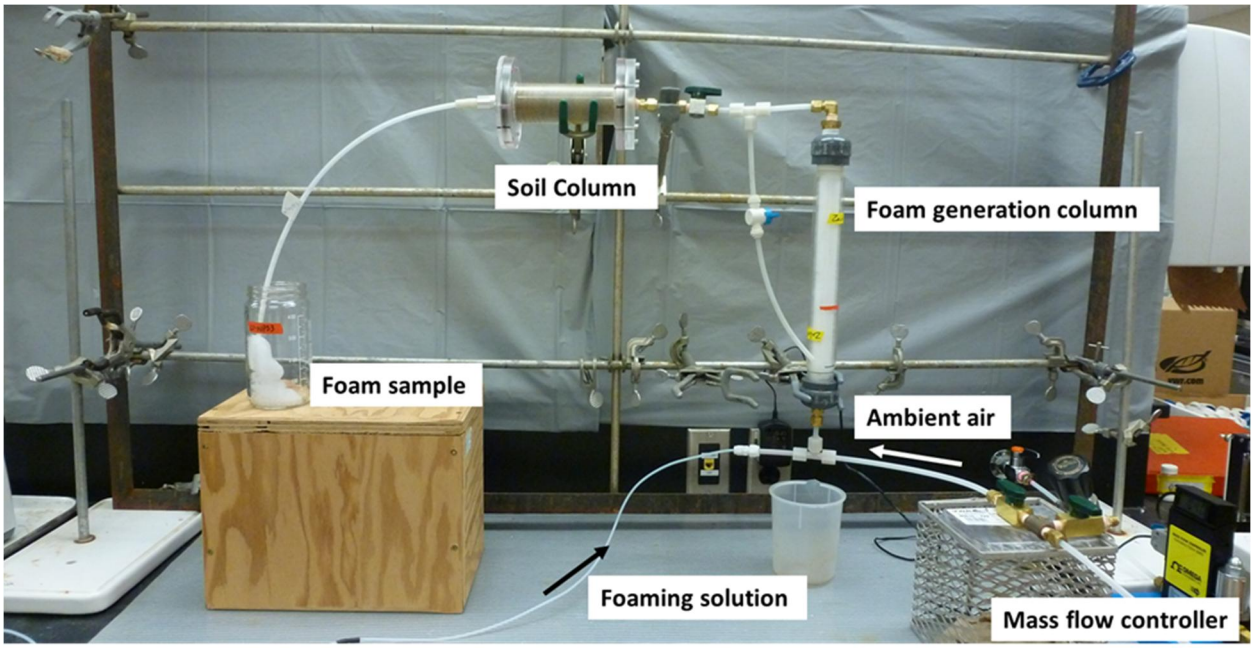

Figure 2.1. The bench-scale foam generation system.

2.5 Effect of ENPs on Foam Properties

A series of experiments were performed to assess the compatibility of the ENPs on foam properties. These investigations focused on gathering information to: (1) determine the potential effect of the surfactants on the foam properties of the ENP-only solution (i.e., the ENPs in an aqueous solution of Pluronic (10 g/L)), and (2) to evaluate whether the foam properties changed in the presence of the ENPs using the Ross Miles Test. The ENP-only solution (500 mg/L) was used to generate foam and the properties of this foam were determined. Foaming solutions were also prepared by mixing the ENP-only solution and the surfactant solution (1:1) to achieve final ENP concentration of 500 mg/L and surfactant concentration of 0.3 wt%. The ENP concentration was selected based on previous research (Linley 2019) and such that it established the analytical procedure for the ENP concentration analysis. The surfactant concentration was selected such that it enabled foam generation for all the surfactants in

Section 2.6 and Section 2.7. The foam properties of the ENP-only solution (500 mg/L) were compared to those of the foaming solutions containing the surfactant and the ENPs to provide insight into item (1) above. Changes in the foamability and stability of each foaming solution due to the presence of the ENPs (item (2) above) were investigated by comparing the behavior of each surfactant to the data collected in the screening tests described in Section 2.3. All experiments were conducted in triplicate.

2.6 Ability of Generated Foams to Support ENPs

The ability of foams generated by the surfactants to support ENPs were investigated by comparing the ENP concentration in foam to that in the foaming solution. The foaming solution and ambient air were introduced to the FG column to generate the foam. Foaming solutions were prepared by adding the ENPs (500 mg/L) and surfactant (0.3 and 0.1 wt%) to MQW. Surfactant concentration of 0.1 wt% was explored as it was used in a subsequent experiment in Section 2.7.

2.7 Column Experiments

Foam only column trials were conducted as preliminary experiments to explore the ability of foam to propagate through unsaturated media. A series of column experiments were then conducted to investigate the capability of foam to transport ENPs in unsaturated media. The impact of surfactant type and concentration, and initial water content of the unsaturated porous medium on the capability of foam to transport the ENPs were investigated. A total of five trials were conducted; four in initially partially saturated media, and one in an initially dry medium. All column experiments were conducted horizontally and conducted at room temperature (22 °C).

Each plexiglass column (15 cm long, 3.5 cm inner diameter) was dry-packed with Borden Sand. Packing was conducted in lifts of 20 ± 2 g, and the side of the column was tapped with a ramrod to settle the sand sediments. Using the base of the ramrod, the sediments were pressed down to ensure it was tightly packed. Then, the side of the column was tapped again. Before the next lift of sand was poured, a metal rod was used to gently disturb the surface of the settled sediments to prevent a thin layer of settled fines from forming. Prior to packing, the sediments were sieved (75 μm stainless steel sieve), washed under running distilled water, and then dried for ~24 h at ~85 °C. After packing, each column was weighed (M_{dry}). To establish an initial volumetric water content ($\theta = 0.2$) in each initially partially saturated column, MQW was flushed from the bottom (0.3 mL/min) until the column was saturated. Then, the column was allowed to drain by applying vacuum (~ 553 mmH_2O) to the bottom of the column. The initial volumetric water content was selected such that it was higher than residual

volumetric water content (θ_r) and lower than saturated volumetric water content (θ_s). The vacuum pressure was selected based on the capillary pressure-saturation (P_c-S_w) relation for Borden aquifer sediments (Neville 1990). After draining, each column was re-weighed ($M_{drained}$). Using the water density and the difference between $M_{drained}$ and M_{dry}, the volume of water that retained in column after draining was calculated. The initial volumetric water content was determined using the volume of retained water divided by the volume of packed zone.

The surfactants selected from the screening tests (Section 2.3) were used at a concentration of 0.3 wt% to generate foam. To assess the effect of surfactant concentration, one of the surfactants was used at a concentration of 0.1 wt% in a partially saturated column trial. For comparison, one ENP transport trial was performed using a porous medium that was an initially dry system.

To establish baseline recovery conditions for ENP mass recovery (defined as the fraction of the total injected ENP mass observed in column effluent), bromide (Br^-, a conservative tracer) was added at a concentration of 100 mg/L along with the ENPs (500 mg/L) to the foaming solution. Foam with the ENPs and Br^- was injected into each column for 150 minutes. The slug injection of the ENPs and Br^- was followed by the injection of foam only. Each experiment was continued for 4.5 to 7.5 h to ensure the ENPs and Br^- were no longer present in column effluent. The injected volume of the ENPs and Br^- was not the same in the trials. The FG column behaved differently in the experiments and caused the solution layer on the porous stone to gradually elevate. This, in turn, negatively affected the foam bubble uniformity (checked by observation) and its continuous generation. To prevent the solution layer from rising, the injection of the foaming solution was adjusted by intermittently turning the pump on and off at various time intervals (from 0 to 15 min as needed). At the conclusion of each trial, the column was weighed (M_{final}) and the difference between M_{final} and $M_{drained}$ for partially saturated columns, and M_{final} and M_{dry} for initially dry column were used to determine liquid uptake.

Foam samples (300 to 500 mL) were continuously collected such that they provided sufficient volume for ENP and Br^- concentration analyses. Br^- concentrations were determined by ion chromatography (IC) with a method detection limit (MDL) of ~0.1 mg/L. An Inductively Coupled Plasma-Orbital Electron Spectrometer (ICP-OES) with a MDL of 4 µg (Fe_T)/L was used to quantify total iron concentration in the effluent samples. Breakthrough curves (BTCs) for the ENP and bromide were generated to assess ENP and bromide transport by foam in column. Mass balance considerations and the BTCs were used to determine ENP and bromide mass rcecovery.

Chapter 3 Results and Discussion

3.1 Surfactant Evaluation

The following criteria were employed in the MCDA: origin of synthesis, health hazard, biodegradability, charge type, CMC, and cost. To highlight the impact of CMC and charge type on the behavior of surfactant as foaming agent and to emphasize the economic aspect of surfactant selection, CMC, charge type, and cost were assigned a higher weight compared to the remaining criteria. Different sets of weights (provided in Appendix B, Table B.1) were used, and swing weight assessment was conducted in each set to evaluate the effect of criterion weight uncertainty on the surfactants.

The surfactant scores were assigned such that they reflected the rank of the surfactants with regard to the relevant criterion (Table 3.1). Rhamnolipids and Bioterge AS-40 were assigned the highest (100) and lowest (0) score for having minimal and severe health hazard, respectively, and the other surfactants were assigned scores such that the differences in the scores showed the differences in the level of hazard. Based on the literature, for a given surfactant as foaming agent, a concentration above the CMC is required. As a result, the lower the CMC is, the less the amount of surfactant that is required and hence, the more economical the surfactant is. Therefore, Ammonyx LO and DHSS were assigned 100 and 0 for CMC as they had the lowest and highest CMC, respectively, and the scores of all other surfactants were scaled between 0 and 100. In terms of cost, Rhamnolipids was assigned 0 as it is the most expensive surfactant. Steol CS-460 and Ammonyx LO are the cheapest surfactants and were assigned 100. For the remaining surfactants, their scores for cost were scaled between 0 and 100 in proportion to the inverse of their costs. With regard to charge type, anionic surfactants are preferred over other surfactants due to the behaviors discussed earlier. Therefore, all surfactants were allocated 100 except Triton X-100 and Ammonyx LO that are not anionic and were allocated 0. In terms of biodegradability, all surfactants were assigned 100 except Triton X-100 and DHSS that are not readily biodegradable and hence, were assigned 0. With respect to origin of synthesis, biosurfactants are preferred over synthetic surfactants and therefore, Rhamnolipids was assigned 100, while the remaining surfactants were assigned 0.

Figure 3.1 shows the overall score for each surfactant. The error bars represent the impact of criterion weight uncertainty on the overall scores. Based on these results, the overall score for Steol SC-460 was the highest (91.3 ± 2.3%). This is attributed to the biodegradability and charge type of Steol SC-460, as well as being the cheapest. The overall score for DHSS was the lowest (43.5± 1.4%), since it has the

highest CMC, is the second most expensive surfactant, and is not readily biodegradable. The overall score for Steol CS-460 was superior to Bioterge AS-40 (91.3% compared 87.8%). Similar to Steol CS-460, Bioterge AS-40 had the highest score for biodegradability and charge type, and is approximately the same cost (Table 2.1); however, it has a significantly higher CMC (~4 times) and is more hazardous.

Table 3.1. Scores of the surfactants on MCDA criteria

Surfactant	Criteria					
	Origin of synthesis	Health Hazard	Biodegradability	Charge Type	CMC	Cost
SDS	0	25	100.0	100.0	84.7	98.3
Steol CS-460	0	50.0	100.0	100.0	99.6	100.0
Bioterge AS-40	0	0	100.0	100.0	98.1	99.9
Triton X-100	0	25	0	0	99.1	98.8
Rhamnolipids	100.0	100.0	100.0	100.0	99.9	0
Ammonyx LO	0	25	100.0	0	100.0	100
DHSS	0	50.0	0	100.0	0	96.9

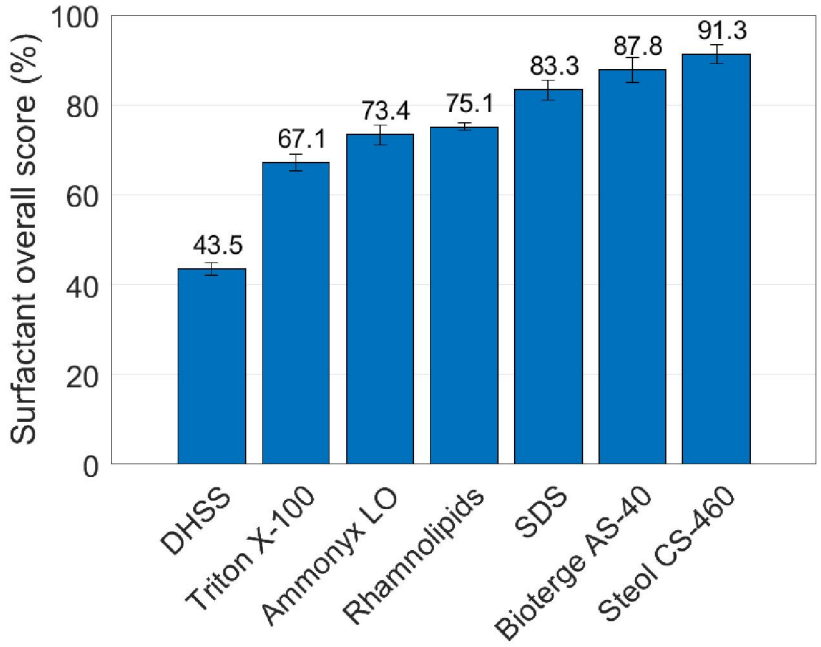

Figure 3.1. Overall score for each surfactant determined by the MCDA.

Figure 3.2 shows the impact of criterion weight on the rank of the surfactants evaluated by the MCDA. The results indicate that the criterion weight uncertainty did not affect the rank for Steol CS-460, Bioterge AS-40, SDS, Triton X-100, and DHSS, for the sets of weights explored. The rank for Rhamnolipids and Ammonyx LO changed, nonetheless, they remained in the rank of 4 to 5 (Figure 3.2). It was demonstrated that DHSS and Triton X-100 had the lowest overall scores among the surfactants. Based on these results, DHSS and Triton X-100 were the least-preferred surfactants, and were not selected for the subsequent foamability and foam stability experiments.

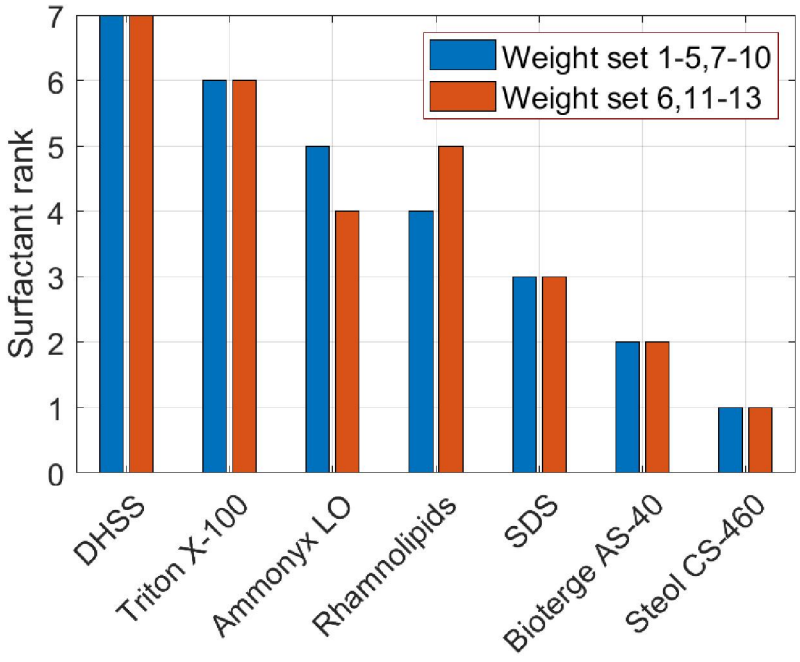

Figure 3.2. Effect of criterion weight uncertainty on the rank of each surfactant. The surfactant ranks shown on the vertical axis are such that a rank of 1 corresponds to the surfactant with the highest score and a rank of 7 corresponds to the surfactant with the lowest score.

3.2 Foamability and Foam Stability

Figure 3.3(a, b) displays the foamability and foam stability for various surfactant concentrations (0.01 to 1.5 wt%) in the screening tests with MQW. As the concentration increased from 0.01 to 0.1 wt% and 0.1 to 1.5 wt%, the foamability of Bioterge As-40 increased by up to 66% and 6%,

respectively. Under the same concentration conditions, the foamability of Steol CS-460 increased by 28% and 7%. Our observation also showed 12% foamability increase for Rhamnolipids when the concentration went from 0.1 to 1.5 wt%. Similar to Bioterge As-40 and Steol CS-460, the foamability of Ammonyx LO and SDS moderately increased with in an increase in the concentration from 0.01 to 0.1 wt% while they slightly increased beyond 0.1 wt%. The results indicate that the influence of surfactant concentration on foamability was less pronounced from 0.1 to 1.5 wt%. The results also demonstrated different foamabilities for the surfactants explored. As shown on Figure 3.3(a), at the same surfactant concentration below 0.1 wt%, Steol CS-460, Bioterge AS-40, and Ammonyx LO had higher foamabilities compared to SDS.

The ratio of concentration to CMC ($C/CMC_{surfactant}$), here called α, was found to affect the concentration dependency of foamability. Indeed, for four surfactants, the change of foamability over the change of concentration ($\Delta foamability/\Delta C$), here called β, was shown to significantly decrease from > 42 cm/wt% to < 3 cm/wt% as α increased above a certain threshold value for each surfactant. These values are: 13.5 for Steol CS-460, 0.4 for SDS, 3.3 for Bioterge AS-40, and 90.9 for Ammonyx LO (Table 3.2). Moreover, it can be seen that β for Ammonyx LO decreased at a higher α (90.9) compared to Steol CS-460 (13.5), SDS (0.4), and Bioterge AS-40 (3.3). SDS generated almost no foam at 0.01 wt%. This observation suggests that the generation of foam by SDS initiates when α is above 0.04.

Table 3.2. Ratio of concentration to CMC for the tested surfactants

Surfactant solution (concentration)	$C/CMC_{surfactant}$
Steol CS-460 (0.1 wt%)	13.5
SDS (0.1 wt%)	0.4
Bioterge AS-40 (0.1 wt%)	3.3
Ammonyx LO (0.1 wt%)	90.9

With an increase in concentration, the stability of the foam generated by Steol CS-460 varied from 94.5 to 99.4% (Figure 3.3(b)). The stability of foam generated by Bioterge AS-40 had a moderate increase from 79.6% at 0.01 wt% to 99.6% at 0.05 wt%. Similar to Steol CS-460, the stability of foam generated by Bioterge AS-40 remained approximately the same (within the range of 96.1 to 100.0%) with an increase in concentration from 0.05 to 1.5 wt%. These results indicate that the increase in surfactant concentration had little to no effect on the stability of foam generated by Steol CS-460 and Bioterge AS-40 within the range of 0.05 to 1.5 wt%. As the concentration increased from 0.1 to 1.5 wt%, the stability of the foams generated by SDS, Rhamnolipids, and Ammonyx LO decreased by 10,

25, and 80%. Previous research has demonstrated that increasing surfactant concentration can lead to decreasing or approximately constant foam stability (Burcik 1950). The marked decrease in the stability of the foam generated by Ammonyx LO is attributed to its higher value of α compared to those of SDS and Rhamnolipids at 0.1 wt%. This observation suggests that within the same concentration range, α can significantly influence the foam stability of different surfactants investigated. The results indicate that for a surfactant concentration above 0.1 wt%, Steol CS-460 and Bioterge AS-40 yielded a higher foam stability compared to Ammonyx LO, Rhamnolipids, and SDS.

Figure 3.3(c, d) shows the foamability and foam stability of the surfactants tested with synthetic groundwater (SGW). Ammonyx LO was not employed in these tests as its foam stability significantly decreased at the concentration range explored in MQW (Figure 3.3(b)). The foamability of Steol CS-460 increased from 14.0 cm at 0.01 wt% to 18.4 cm at 1.5 wt%. The foamability of Rhamnolipids and SDS decreased slightly by 3% when SGW was used. These results demonstrate that the foamability of Steol CS-460, Rhamnolipids, and SDS were approximately the same, using SGW or MQW. The foamability of Bioterge AS-40 decreased by 17% at 0.01 wt%, and increased by 6% within the concentration range of 0.05 to 1.5 wt% when SGW was used. This indicates that the SGW had little effect on Bioterge AS-40 foamability above 0.05 wt%. It was observed that the use of SGW changed the foam stability of Steol CS-460, Bioterge AS-40, and SDS by 5%. The stability of foam generated by Rhamnolipids increased slightly by 2% at 0.1 wt%, and 12% at 1.5 wt%. Overall, these results suggest that the SGW had little effect on the foamability and foam stability of the surfactants investigated at the concentration range explored.

When the surfactant concentration increased, foamability increased. The effect of surfactant concentration on foamability was less pronounced above 0.1 wt%. At the same surfactant concentration, Steol CS-460, Bioterge AS-40, and Ammonyx LO had a higher foamability compared to SDS and Rhamnolipids. It was also demonstrated that for a surfactant concentration above 0.1 wt%, the foam stability was approximately the same for Steol CS-460 and Bioterge As-40 while it decreased for Ammonyx LO, Rhamnolipids, and SDS. At the surfactant concentration range explored (0.1 to 1.5 wt%), Steol CS-460 and Bioterge AS-40 yielded a higher foam stability compared to Ammonyx LO, Rhamnolipids, and SDS. Based on these findings, Steol CS-460 and Bioterge As-40 showed the highest foamability and foam stability and were only slightly affected by the SGW over the concentration range from 0.1 to 1.5 wt% and hence, were selected for the subsequent experimental efforts. Ammonyx LO was also used for comparison purposes.

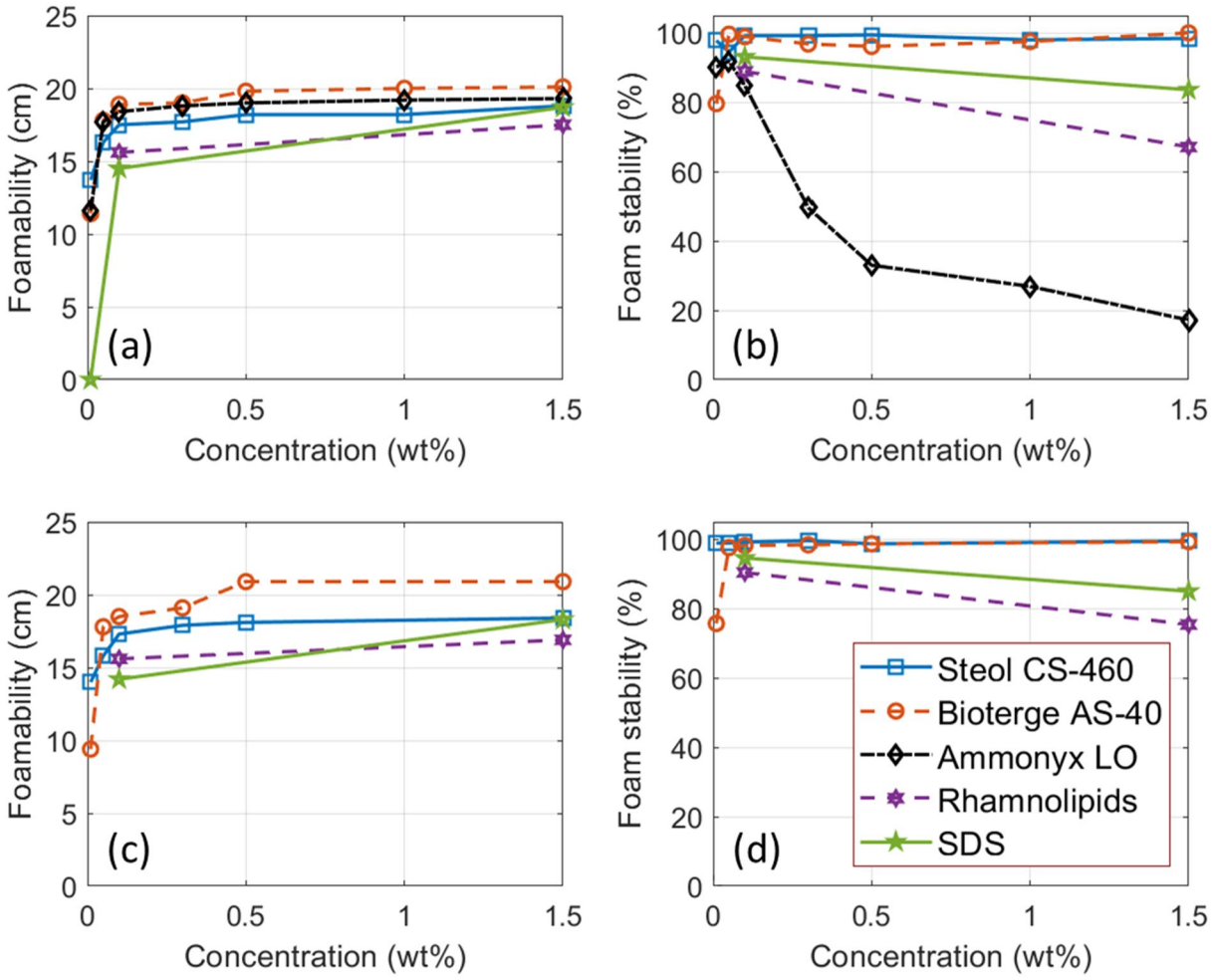

Figure 3.3. Effect of surfactant type and concentration on foamability and foam stability in tests conducted with MQW (a, b) and SGW (c, d).

3.3 ENP Concentration in Foam

The concentration of the ENPs in the foam generated by Steol CS-460 (0.1 and 0.3 wt%), Bioterge As-40 (0.3 wt%), and Ammonyx LO (0.3 wt%) were between 97% ± 1% and 110% ± 1% of the concentration in the foaming solution (Table 3.3). The values over 100% may be due to equipment error associated with the ICP-OES, and human errors during sample dilution for the concentration

analysis. The results demonstrate that the ENP concentration in the foaming solution was maintained by the FG column. This, in turn, indicates that the generated foams were able to support the ENPs.

Table 3.3. Ability of generated foams to support the ENPs

Surfactant solution (concentration)	$C_{ENP,foam}/C_{ENP,solution}$ (%)
Steol CS-460 (0.3 wt%)	102 ± 1
Steol CS-460 (0.1 wt%)	99 ± 1
Bioterge AS-40 (0.3 wt%)	110 ± 1
Ammonyx LO (0.3 wt%)	97 ± 1

3.4 Foamability and Foam Stability in the Presence of ENPs

Figure 3.4(a, b) displays the foamability and foam stability of the ENP-only solution (500 mg/L), and the surfactant solutions in the presence and absence of the ENPs. Based on the results of paired t-test, the foamability of Steol CS-460, Bioterge AS-40, or Ammonyx LO in the presence of the ENPs was statistically higher than that of the ENP-only solution (5% LOS). This indicates that the surfactants significantly enhanced the ability of the ENP-only solution to generate foam. It was also observed that the foam stability of the ENP-only solution was increased from 72.8% to 90.5% and 98.4% when Steol CS-460 or Bioterge AS-40 were added to the foaming solution, respectively. Since the ENPs are in an aqueous solution of Pluronic, it might be that adding Steol CS-460 or Bioterge AS-40 to Pluronic led to a synergistic effect that lowered the interfacial tension between the liquid and air. Unlike Steol CS-460 and Bioterge AS-40, Ammonyx LO did not noticeably change the foam stability of the ENP-only solution.

The ENPs were found to affect the foamability and foam stability of the investigated surfactants. Our observation shows that the stability of the Steol CS-460 foam slightly decreased from 99.2 to 90.5% when the ENP-only solution was added to the foaming solution. The foamability of Bioterge AS-40 remained approximately unchanged as the ENP-only solution was added to the foaming solution, whereas the stability of the generated foam slightly increased from 96.8% to 98.4%. A paired t-test shows that the foamability and foam stability of Ammonyx LO (20.0 ± 0.1 cm and 72.0 ± 3.8%) in the presence of the ENPs were statistically higher than those (18.8 ± 0.1 cm and 49.5 ± 0.3%) in the absence of the ENPs (5% LOS). These observations suggest that the mixture of Pluronic with either Ammonyx LO or Bioterge AS-40 lowered the interfacial tension between the liquid and air compared to when Ammonyx LO or Bioterge AS-40 were the only surfactant present in the foaming solution. The addition

of nanoparticles has been shown to enhance foam stability by decreasing bubble drainage and coalescence (Sun et al. 2014).

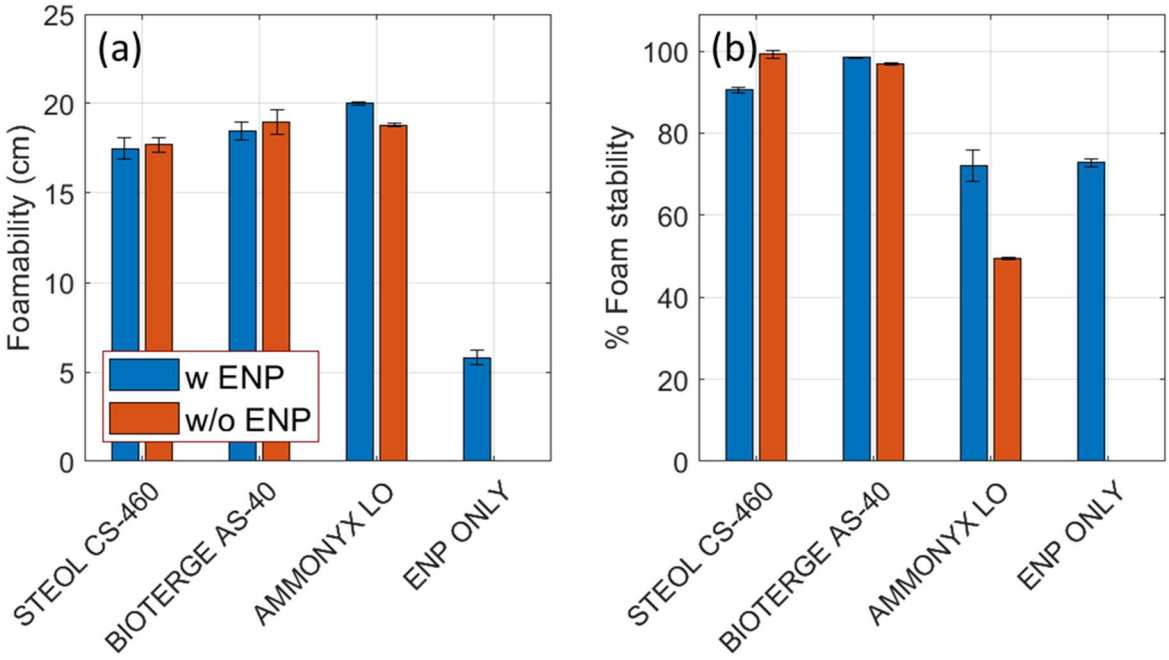

Figure 3.4. Foamability (a) and foam stability (b) of Steol CS-460, Bioterge AS-40, and Ammonyx LO in the presence and absence of the ENPs, and the ENP-only solution.

3.5 Transport of ENPs using Foam

3.5.1 General Observations

The operational parameters for the five column experiments are listed in Table 3.4. The lack of accuracy in the ENP and tracer concentrations is possibly due to equipment error associated with the ICP-OES, the graduated cylinder, and the pipettes that were used to prepare solution dilutions. The injected solution volume was not the same in all trials due to the different time intervals (0 to 15 min). Consequently, the injected ENP mass was also not similar in all trials. Here, the average foam inflow rate was considered to be the rate at which the solution and air were injected. The initial volumetric water content (ɵ) in each partially saturated column was calculated using the volume of retained water in column divided by the volume of packed zone. The differences in the values of ɵ in the trials except Trial-3 is due to the slight differences in vacuum duration (~1.5 h) in the trials.

Table 3.4. Operational parameters of column experiments

Column ID	ENP influent concentration (mg/L)	Tracer influent concentration (mg/L)	Injected solution volume (ENPs + Br^-) (mL)	Injected foam volume (ENPs + Br^-) (mL)	Average foam inflow rate (mL/min)	Total injected ENP mass (mg)	Surfactant	Surfactant concentration (wt%)	Initial volumetric water content (ɵ)
Trial-1	491	91	92	6120	40.8	45.2	Steol CS-460	0.3	0.20
Trial-2	486	82	57	6105	40.7	27.7	Steol CS-460	0.1	0.22
Trial-3	532	84	54	6105	40.7	28.7	Steol CS-460	0.3	0 (dry)
Trial-4	509	83	94	6105	40.7	47.8	Bioterge AS-40	0.3	0.23
Trial-5	453	73	38	6045	40.3	17.2	Ammonyx LO	0.3	0.18

When the foam bubbles entered the column, bubble film rupture occurred, the gas phase was released, and the liquid phase (i.e., ruptured film) including the ENPs and bromide was retained in the pore spaces. As a result of film rupture, liquid-only effluent exited the column prior to the foam bubbles. The bubbles started regenerating and appeared in the effluent when water saturation in the column increased to a critical saturation, which is defined as the water saturation below which bubble film rupture is inevitable in porous media (Zhong et al. 2010). In all trials, air gaps were observed when the first effluent (i.e., liquid only) exited the column. Then, a mixture of liquid and foam bubbles gradually started exiting the column. The air gaps caused discontinuities in the effluent foam flow resulting in larger bubbles (diameter > 1 cm) that collapsed soon after they exited the column. The air gaps confirm that film rupture occurred as the foam bubbles were transported through the column. Once the first foam-only effluent appeared, the air gaps disappeared in all trials, except Trial-2 and Trial-5 where the air gaps still persisted.

In Trial-5, the effluent air gaps were larger than those in Trial-2 and did not diminish for the entire experiment and hence, caused discontinuities in the effluent foam flow. As a result, there existed larger foam bubbles in the effluent that tended to collapse sooner compared to those in the other trials. This could be attributed to the charge type of Ammonyx LO. As a zwitterionic surfactant, Ammonyx LO carries both a positive and a negative charge as opposed to Steol CS-460 and Bioterge AS-40 that are anionic surfactants and carry only negative charge. Due to the negative surface charge of the soil media, an electrostatic attraction may occur between Ammonyx LO and the soil surface, leading to the adsorption of Ammonyx LO to the soil surface. This, in turn, results in the loss of available mass of Ammonyx LO, causing film rupture in the generated foam. The observations suggest that the bubbles in Trial-5 had the lowest stability within the porous medium compared to the other trials as the stability of foam depends on film rupture (Wang and Li 2016).

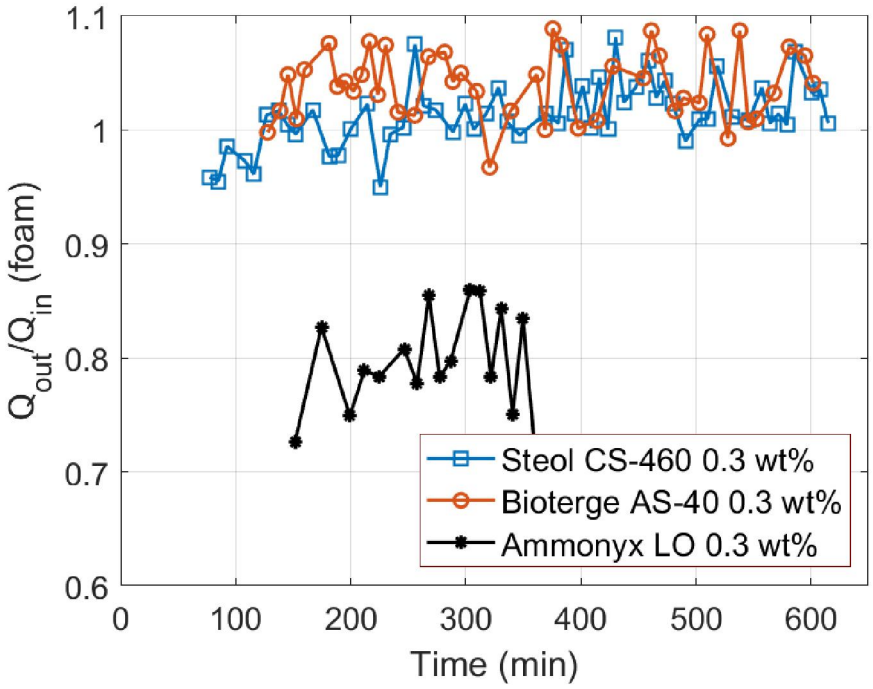

Figure 3.5. Ratio of foam outflow rate (Q_{out}) to average foam inflow rate (Q_{in}).

Figure 3.5 displays the ratio of the foam outflow rate (defined as foam sample volume divided by sample collection time) to the average foam inflow rate (referred to as foam flow ratio) for Trial-1, Trial-4, and Trial-5. Trial-5 has the lowest foam flow ratio due to the discontinuity in the effluent foam

flow, as well as the lower foam stability of Ammonyx LO compared to Steol CS-460 and Bioterge AS-40. The foam flow ratios in Trial-1 and Trial-4 were 1.01 ± 0.03 and 1.04 ± 0.03, respectively. The values of foam flow ratio above unity were unexpected and are due to erroneous sample volume measurement. The effluent foam volume was directly read from the graduation mark on the volumetric sample bottle which was approximate.

3.5.2 ENP and Tracer Breakthrough Behaviour and Mass Recoveries

Figure 3.6 shows the ENP and Br^- breakthrough curves (BTCs) for all experimental trials. For quantitative visual comparison of BTC data, the time of the BTCs are normalized to the time of the occurrence of center of mass (t_c) (defined as the time by which half of the injected mass transported in column) of Br^-. Except Trial-5, the ENP effluent concentration rose sharply to values approximately equal to or greater than the influent concentration (C/C_o <1.20) (the rising limb) and then, decreased to very low values following the end of the ENP injection ($C/C_o \leq 0.02$) (the falling limb). The normalized ENP and Br^- BTCs above unity, particularly for Trial-4 were unexpected and may be a result of experimental and human errors during experimental setup, execution, or sample preparation (e.g. sample dilution) for the ENP and Br^- concentration analyses. It is also possible that evaporation occurred during the sample preparation or analysis operation, leading to sample loss and subsequently, the ENP and Br^- concentrations higher than the influent concentration. Br^- was expected to behave conservatively, and the ENP effluent concentration was not expected to exceed the influent concentration as there was initially no ENPs in columns. The normalized ENP mass recoveries were determined to quantify the ENPs that transported in column for all trials, and tracer mass recoveries were also calculated for comparison purposes (Figure 3.7). The ENP recovery in Trial-1 (101%) and tracer recovery in Trial-5 (105%) are slightly over 100%, possibly due to human and experimental errors in sample volume measurement and sample preparation for the ENP and Br^- concentration analyses.

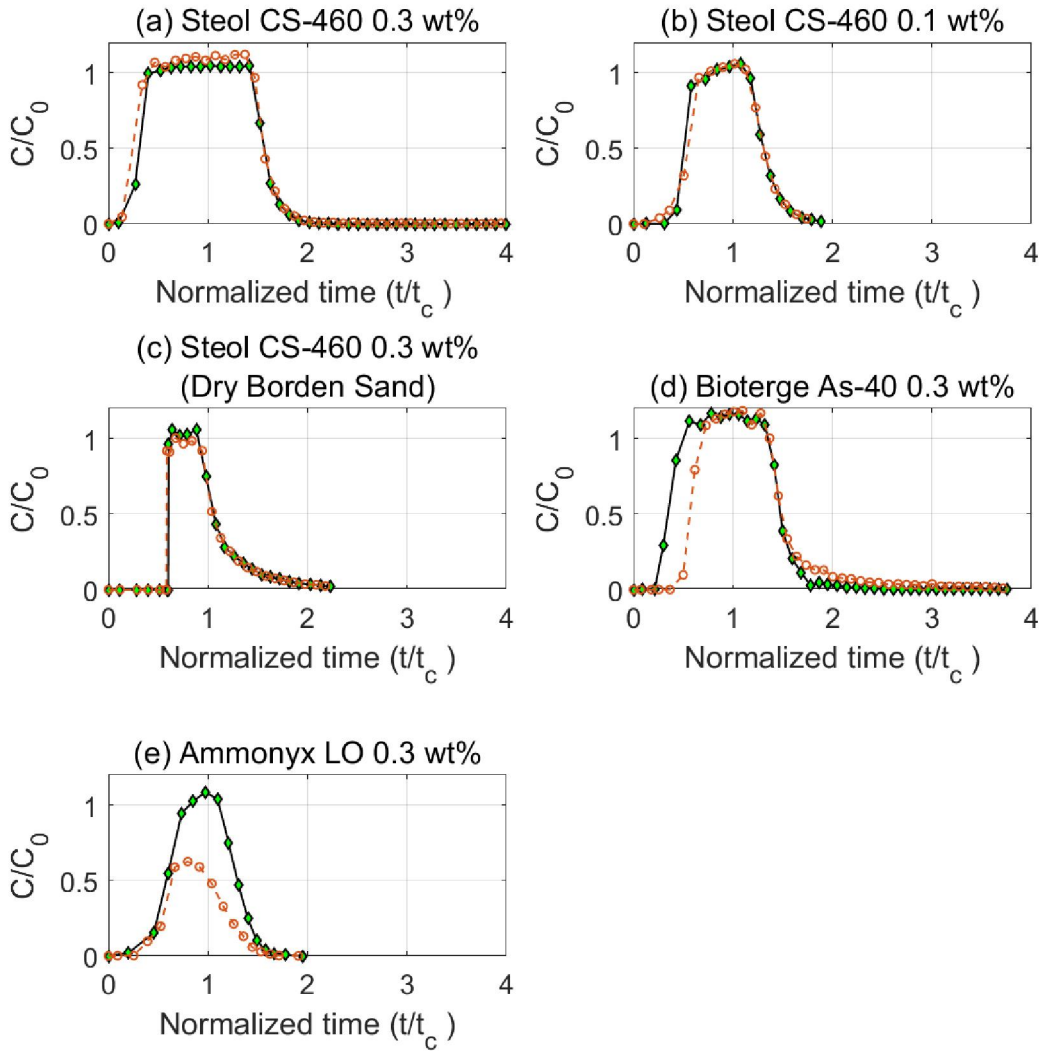

Figure 3.6. ENP (open circle symbols) and Br^- (solid diamond symbols) breakthrough curves for Trial-1 (a), Trial-2 (b), Trial-3 (c), Trial-4 (d), and Trial-5 (e). The horizontal axis shows time normalized to the Br^- t_c.

In Trial-1, Trial-2, and Trial-3, the BTCs of the ENPs and Br^- were approximately similar with regard to their shape and the normalized time of the peak effluent concentration ($(t/t_c)_{peak}$), demonstrating no preferential ENP attachment to the sediments compared to the conservative tracer. These observations

indicate that the average transport velocity (defined as column length divided by t_c) of the ENP in these trials was equal to that of Br^- and is consistent with the result that the ENP recoveries were approximately equivalent to Br^- recoveries. It should be noted that the injected ENP mass in Trial-2 and Trial-3 was approximately half of that in Trial-1, however, the ENP recovery remained essentially unchanged when the concentration of Steol CS-460 was decreased from 0.3 wt% in Trial-1 to 0.1 wt% in Trial-2. These results demonstrate that the foam generated by Steol CS-460 at 0.3 or 0.1 wt% was capable to transport the ENPs in the unsaturated porous media (≥ 95% ENP recovery). The ENP and Br^- recovery slightly decreased from 101 and 95% for a system with an initial volumetric water content of 0.2 in Trial-1 to 89 and 90% in an initially dry system in Trial-3. This is thought to be due to the ENP and Br^- entrapment in immobile air-water interfaces. This interpretation is supported by the observed asymmetrical and well-matched shapes of the ENP and BTCs (DeNovio et al. 2004; Prédélus et al. 2017). Although zero water content is not possible *in situ*, the result implies that foam generated by Steol CS-460 is capable to transport the ENPs in dry porous media.

In Trial-4, the rising limb of the ENP BTC was delayed relative to that of the Br^- BTC and the ENP ($(t/t_c)_{peak}$) was greater than Br^- ($(t/t_c)_{peak}$), indicating the ENP attachment and detachment to the sediments, particularly evidenced by the ENP BTC tailing. As a result, the ENP average transport velocity (0.078 cm/min) was smaller compared to that of Br^- (0.095 cm/min). The ENP recovery (93%) is slightly lower than Br^- recovery (100%). It is possible that if Bioterge AS-40 associated with the ENPs in foam, the surface properties would change and the ENPs would be more susceptible to retention in the packed column. The injected ENP mass in Trial-1 and Trial-4 was approximately the same, however the ENP recovery in Trial-4 (93%) was slightly lower than that in Trial-1 (101%). This result and the observed ENP and Br^- BTCs suggest that for the same surfactant concentration, the foam generated by Steol CS-460, as opposed to Bioterge AS-40, behaved almost conservatively (i.e., little or no interaction with the sediments).

The ENP BTC in Trial-5 did not match Br^- BTC, and the peak of ENP BTC (0.63) was markedly lower than that of Br^- BTC (1.09). These observations and the significantly lower ENP recovery (54%) compared to Br^- recovery (105%) suggest that the foam generated by Ammonyx LO resulted in the attachment of the ENPs to the sediments. This may be attributed to the alteration of the surface charge of the ENPs due to the presence of Ammonyx LO. As a zwitterionic surfactant, Ammonyx LO carries both a positive and a negative charge. The hydrophobic domains of Ammonyx may adsorb to the hydrophobic surface of the Pluronic-coated ENPs, producing a particle structure containing both

positive and negative electrostatic charges at its surface. Owing to the surface characteristics of the soil media, which exhibits an overall negative charge, the zwitterionic ENPs may experience an electrostatic attraction resulting in physisorption of the ENPs to the soil (Harwell et al. 1999; Yan et al. 2012; Singh and Misra 2016). This suggests that the foam generated by Ammonyx LO led to ENP retention.

The total mass of column in Trial-1 and Trial-4 remained approximately unchanged ($M_{final} \approx M_{drained}$) (i.e., no liquid uptake), however, the column mass increased in Trial.5 (liquid uptake = 7.5 ± 0.5 g). This increase is attributed to the higher film rupture of Ammonyx LO foam bubbles compared to Steol CS-460 and Bioterge AS-40 foam bubbles. As a result, more bubbles collapsed compared to the regenerated bubbles within the porous medium in Trial-5, and the liquid phase associated with the bubbles was retained in the column, leading to an increase in mass. This observation supports the lower stability of the foam generated by Ammonyx LO compared to the foams generated by Steol CS-460 and Bioterge AS-40 discussed earlier.

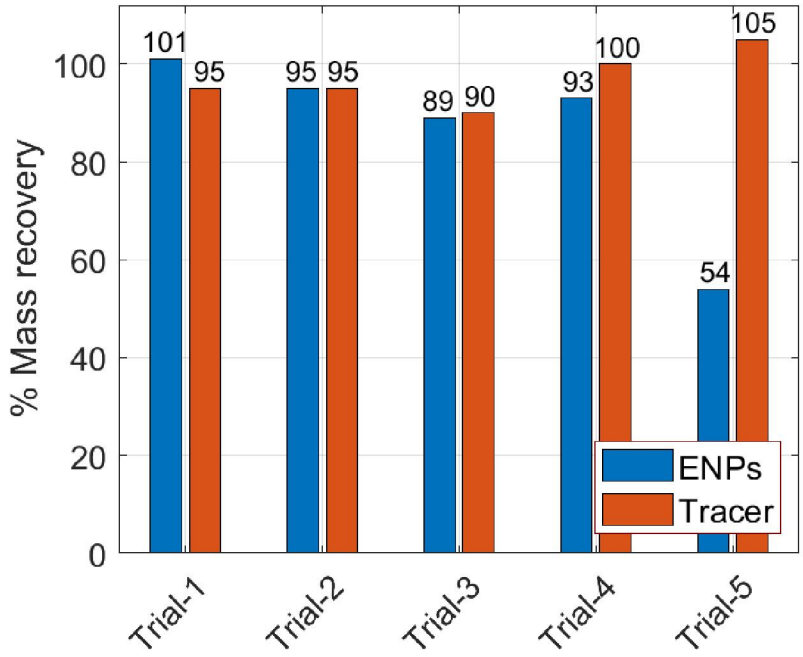

Figure 3.7. ENP and tracer mass recovery for each trial.

Chapter 4
Conclusions and Recommendations

4.1 Conclusions

The research conducted in this thesis contributes to the knowledge dealing with ENP transport by foam in the unsaturated zone. To this end, the compatibility of the ENPs on foam properties (i.e., foamability and foam stability) and the capability of foam to deliver the ENPs in unsaturated media were investigated. These evaluations were achieved through foamability and foam stability experiments using the Ross Miles method and column transport studies. Prior to these experiments, a MCDA and foamability and foam stability experiments were conducted to select foaming agents (surfactants) for subsequent experimental efforts.

Based on the MCDA results, Steol CS-460, Bioterge AS-40, SDS, Ammonyx LO, and Rhamnolipids were selected to conduct foamability and foam stability experiments. In experiments conducted with MQW, the foamability and foam stability were affected by surfactant type and concentration. As the surfactant concentration increased for a given surfactant, so did the foamability. It was demonstrated that the effect of surfactant concentration on foamability was less marked above 0.1 wt% at the concentration range explored. It was also observed that the ratio of surfactant concentration to CMC (α) played a role in foamability. Above 0.1 wt%, the change of foamability over the change of concentration decreased at a higher α for Ammonyx LO compared to Steol CS-460, SDS, and Bioterge AS-40. The foam stability of Ammonyx LO, Rhamnolipids, and SDS decreased as the surfactant concentration increased above 0.1 wt%, however, for the same concentration the stability of Steol CS-460 and Bioterge As-40 foams remained essentially unchanged. For a surfactant concentration between 0.1 and 1.5 wt%, Steol CS-460 and Bioterge AS-40 had higher foam stabilities compared to those of Ammonyx LO, Rhamnolipids, and SDS. It was observed that the foamability of Steol CS-460, Rhamnolipids, and SDS remained unchanged using SGW compared to MQW. The foamability of Bioterge AS-40 slightly decreased at 0.01 wt% and was not affected above a concentration of 0.05 wt%. SGW was also found to have little effect on the foam stability of Steol CS-460, Bioterge As-40, and SDS. The foam stability of Rhamnolipids remained the same at 0.1 wt% and slightly increased at 1.5 wt% when the SGW was used. These observations indicate that the SGW had little to no effect on the foamability and foam stability of the surfactants within the concentration range explored except for Bioterge As-40 foamability at 0.01 wt% and Rhamnolipids foam stability at 1.5 wt%.

Foams generated by Steol CS-460, Bioterge AS-40, and Ammonyx LO showed the ability to support the ENPs. The effect of Steol CS-460, Bioterge AS-40, and Ammonyx LO on the foamability and foam stability of the ENP-only solution was demonstrated, and it was observed that Steol CS-460, Bioterge AS-40, and Ammonyx LO enhanced the foamability of the ENP-only solution. Steol CS-460 and Bioterge AS-40 improved the foam stability of the ENP-only solution, while Ammonyx LO did not noticeably change it. The impact of the ENPs on the foamability and foam stability of the surfactants was also investigated. The ENPs improved the foamability and stability of the generated foam by Ammonyx LO. Also, the foam stability of Bioterge AS-40 increased, and its foamability did not noticeably change in the presence of the ENPs. Moreover, the foamability of Steol CS-460 remained approximately unchanged, whereas its foam stability slightly decreased from 99.2% ± 0.9% to 90.5% ± 0.7% when the ENPs were added to the foaming solution. These results imply that the ENPs are compatible with the foamability of the surfactants and the foam stability of Bioterge AS-40 and Ammonyx LO.

Column experiments were conducted to determine the potential for foam generated by Steol CS-460, Bioterge AS-40, and Ammonyx LO to transport the ENPs in unsaturated porous medium. The impact of surfactant type and concentration, and initial volumetric water content on the ENP transport by foam was investigated. The foam generated by Steol CS-460 led to a slightly higher ENP mass recovery (101%) compared to that (93%) when the foam generated by Bioterge AS-40 was used. Besides, the Bioterge AS-40 foam delayed the ENP transport relative to the tracer. Also, the foam generated by Ammonyx LO resulted in a significantly lower ENP mass recovery (54%) compared to the tracer mass recovery (105%). These results suggest the ENP attachment to the sediments when the foam generated by Bioterge AS-40 or Ammonyx LO were used. The stability of the foam generated by Ammonyx LO within the porous medium was lower than that of Steol CS-460 and Bioterge AS-40. This finding was supported by the observation of liquid uptake in column when the Ammonyx LO foam was used. It was also demonstrated that the ratio of foam outflow rate to the average foam inflow rate (foam flow ratio) for Steol CS-460 and Bioterge AS-40 was higher than that for Ammonyx LO. This is attributed to the discontinuity in the effluent foam flow, as well as the lower foam stability of Ammonyx LO within the porous medium compared to Steol CS-460 and Bioterge AS-40. Taken together, these findings emphasize the impact of surfactant type on the ENP transport. It was observed that the ENP mass recovery was not materially affected by the concentration of Steol CS-460. Lowering the Steol CS-460 concentration from 0.3 to 0.1 wt% had little to no effect on the ENP mass recovery and did not change the ENP average transport velocity relative to the tracer. As the initial volumetric water content

was decreased (from 0.2 to dry condition), the ENP and tracer mass recoveries slightly decreased, suggesting the ENP and tracer entrapment in immobile air-water interfaces. It should be noted that zero water content is not possible *in situ*, nonetheless, the result implies that foam generated by Steol CS-460 is capable to transport the ENPs in dry porous media. Overall, the results of the column experiments show that the foam generated by Steol CS-460 at a concentration of 0.3 and 0.1 wt% was successfully capable to deliver the ENPs in unsaturated porous media, and thus foam has the potential to deliver the ENPs *in situ*. Bioterge AS-40 and Ammonyx LO demonstrated a lower capability for ENP transport compared to Steol CS-460.

4.2 Recommendations

Although important conclusions were made at the end of this research, there are opportunities for further research which are as follow:

- The injected volume of solution and consequently, the injected ENP mass was not the same in the column trials due to the discrepancies in the behaviour of the foam generation column. Thus, as a future task, the enhancement of the design of the foam generation column, particularly the porous stone, is recommended to enable the injection of a predetermined volume of solution.
- To better understand the effect of surfactant adsorption to the soil media on foam bubble collapse, it is recommended to investigate the adsorption of Steol CS-460, Bioterge AS-40, and Ammonyx LO to the surface of the soil media under batch conditions. These tests may be beneficial as they assess the interaction of the surfactants with the sediments in the absence of the foam bubbles.
- It is also recommended to conduct batch binding tests to further investigate the ENP attachment to Borden sand in the presence of Steol CS-460, Bioterge AS-40, and Ammonyx LO. The transport results seen in this research suggest that Bioterge AS-40 and Ammonyx LO caused the ENPs to attach to the soil media, while Steol CS-460 experienced little or no interaction with the soil. Batch binding tests could evaluate whether this occurs without particle removal in the column, leaving only physisorption interactions to be responsible for ENP retention.
- Further replications are recommended for Trial-1 and Trial-5 in the column experiments to determine a more reliable/accurate mass recovery for the ENPs and tracer. The reported ENP

mass recovery in Trial-1 and tracer recovery in Trial-5 are above 100% and were perhaps due to errors in sample volume measurement and sample preparation for the ENP and tracer concentration analyses. Experimental replications could be beneficial to properly assess the importance of such errors.

- The foamability and foam stability results suggest that: one, Pluronic lowered the interfacial tension of Ammonyx LO or Bioterge AS-40 solution, and two, the mixture of either Steol CS-460 or Bioterge AS-40 with Pluronic lowered the interfacial tension compared to Pluronic. Further research is required to determine such interfacial tensions.
- It is recommended to simulate the ENP and tracer breakthrough curve results in a 1-D model to verify and develop a predictive model.
- Further column experiments are recommended to investigate the capability of foam to deliver binding ENPs (Linley 2019) in LNAPL-contaminated soils.

Bibliography

1. Agarwal, A., & Liu, Yu. (2015). Remediation technologies for oil-contaminated sediments, *Marine Pollution Bulletin*, 101(2), 483-490.
2. American Society for Testing and Materials (ASTM). (2015). Standard Test Method for Foaming Properties of Surface-Active Agents, Designation: D1173 – 07.
3. Bertin, H.J. Apaydin, O.G. Castanier, L.M. & Kovscek, A.R. (1998). Foam Flow in Heterogeneous Porous Media: Effect of Crossflow. Society of Petroleum Engineers, Inc.
4. Burcik, E.J. (1950). The rate of surface tension lowering and its role in foaming. *Journal of Colloid Science*, *5*(5), 421-436.
5. Couto, H. J. B. Massarani, G. Biscaia Jr., E. C. & Sant'Anna Jr., G. L. (2009). Remediation of sandy soils using surfactant solutions and foams. *Journal of Hazardous Materials*, 164(2–3), 1325–1334. http://doi.org/10.1016/j.jhazmat.2008.09.129
6. Crane, R.A. & Scott, T.B., (2012). Nanoscale zero-valent iron: Future prospects for an emerging water treatment technology. *Journal of Hazardous Materials*, 211–212, pp.112–125. Available at: http://dx.doi.org/10.1016/j.jhazmat.2011.11.073.
7. Cytec. (2013). Cytec Industries Incorporated. https://www.solvay.com/en
8. Da Rosa, C. F. C., Freire, D. M. G., & Ferraz, H. C. (2015). Biosurfactant microfoam: Application in the removal of pollutants from soil. *Journal of Environmental Chemical Engineering*, 3(1), 89–94. http://doi.org/10.1016/j.jece.2014.12.008
9. Dickinson, E., & Izgi, E. (1996). Foam stabilization by protein-polysaccharide complexes. *Colloids and Surfaces A: Physicochemical and Engineering Aspects*, 113(1), 191–201.
10. Del Campo Estrada, E., Bertin, H., & Atteia, O. (2015). Experimental Study of Foam Flow in Sand Columns: Surfactant Choice and Resistance Factor Measurement. *Transport in Porous Media*, 108(2), 335–354. http://doi.org/10.1007/s11242-015-0479-8
11. Ding, Y. Liu, B. Shen, X. Zhong, L. & Li, X. (2013). Foam-Assisted Delivery of Nanoscale Zero Valent Iron in Porous Media. *Journal of Environmental Engineering*. 139(September), pp.1206–1212.
12. Dodgson, J. S., Spackman, M., Pearman, A., & Phillips, L. D. (2009). Multi-criteria analysis: a manual.
13. Denovio, N.M., Saiers, J.E. & Ryan, J.N., (2004). Colloid Movement in Unsaturated Porous Media: Recent Advances and Future Directions. *Vadose Zone Journal*, *3*(2), 338-351.
14. Environmental Protection Agency (EPA). (2012). Petroleum hydrocarbons and chlorinated solvents differ in their potential for vapor intrusion, Office of Underground Storage Tanks, Washington, D.C. 20460.
15. Hegge, A. B., Andersen, T., Melvik, J. E., Kristensen, S., & Tønnesen, H. H. (2010). Evaluation of Novel Alginate Foams as Drug Delivery Systems in Antimicrobial Photodynamic Therapy (aPDT) of Infected Wounds — An In Vitro Study: Studies on Curcumin and Curcuminoides XL, 99(8), 3499–3513.
16. Harwell, J. H., Sabatini, D. A., & Knox, R. C. (1999). Surfactants for ground water remediation. *Colloids and Surfaces A: Physicochemical and Engineering Aspects*, 151, 255–268.
17. Huang, C. Van Benschoten, J.E. Healy, T.C. & Ryan, M.E. (1997). Feasibility study of surfactant use for remediation of organic and metal contaminated soils. *Soil and Sediment Contamination*, 6:5, 537-556.
18. Hirasaki, G. J., Miller, C. A., Szafranski, R., Tanzil, D., Lawson, J. B., Meinardus, H., Jin, M., Londergan, J. T., Jackson, R. E., Pope, G. A., & Wade, W. H. (1997). Field Demonstration of

the Surfactant/Foam Process for Aquifer Remediation. *Society of Petroleum Engineers.* http://doi.org/10.2118/39292-MS
19. Jeong, S. W., Corapcioglu, M. Y., & Roosevelt, S. E. (2000). Micromodel study of surfactant foam remediation of residual trichloroethylene. *Environmental Science and Technology*, 34(16), 3456–3461. http://doi.org/10.1021/es9910558
20. Kuppusamy, S., Palanisami, T., Megharaj, M., Venkateswarlu, K., & Naidu, R. (2016). *Reviews of Environmental Contamination and Toxicology*, 236.
21. Karn, B., Kuiken, T., & Otto, M. (2009). Nanotechnology and in Situ Remediation: A Review of the Benefits and Potential Risks. *Environmental Health Perspectives.* 117(12), pp.1823–1831.
22. Kovscek, A. R., & Bertin, H. J. (2003). Foam Mobility in Heterogeneous Porous Media (I: Scaling Concepts). *Transport in Porous Media*, 52, 17–35. http://doi.org/10.1023/A:1022368228594
23. Lees, R., & Jackson, E. B. (1973). Sugar Confectionery and Chocolate Manufacture. Leonard Hill Books, Alesbury, UK.
24. Linley, S. (2019). Polymeric Coatings for Targeted Nanoparticle Delivery to Subsurface Contaminants (Doctoral dissertation). Retrieved from UWSpace. http://hdl.handle.net/10012/14608
25. Linley, S., Holmes, A., Leshuk, T., Nafo, W., Thomson, N.R., Al-Mayah, A., McVey, K., Sra, K., & Gu, F. (2019). Targeted nanoparticle binding & detection in petroleum hydrocarbon impacted porous media. *Chemosphere*, 215, pp.353–361. Available at: https://doi.org/10.1016/j.chemosphere.2018.10.046.
26. Longpre-Girard, M., Martel, R., Robert, T., Lefebvre, R., & Lauzon, J.-M. (2016). 2D sandbox experiments of surfactant foams for mobility control and enhanced LNAPL recovery in layered soils. *Journal of Contaminant Hydrology*, 193, 63–73. http://doi.org/10.1016/j.jconhyd.2016.09.001
27. Lee, B. C., Lee, J., Cheon, J., & Lee, K. (2001). Attenuation of petroleum hydrocarbons in smear zones: a case study, 127(July), 639–647.
28. Mulligan, C. N., Yong, R. N., & Gibbs, B. F. (2001). Heavy metal removal from sediments by biosurfactants. *Journal of Hazardous Materials*, 85(1–2), 111–125. http://doi.org/10.1016/S0304-3894(01)00224-2
29. Mulligan, C. N., & Eftekhari, F. (2003). Remediation with surfactant foam of PCP-contaminated soil. *Engineering Geology*, 70(3-4), 269–279. http://doi.org/10.1016/S0013-7952(03)00095-4
30. Mulligan, C. N., & Wang, S. (2006). Remediation of a heavy metal-contaminated soil by a rhamnolipid foam. *Engineering Geology*, 85, 75–81. http://doi.org/10.1016/j.enggeo.2005.09.029
31. Maire, J., & Fatin-Rouge, N. (2017). Surfactant foam flushing for in situ removal of DNAPLs in shallow soils. *Journal of Hazardous Materials*, 321, 247–255. http://doi.org/10.1016/j.jhazmat.2016.09.017
32. Maire, J., Coyer, A., & Fatin-Rouge, N. (2015). Surfactant foam technology for in situ removal of heavy chlorinated compounds-DNAPLs. *Journal of Hazardous Materials*, 299, 630–638. http://doi.org/10.1016/j.jhazmat.2015.07.071
33. Middeldorp, P. J. M., van Aalst, M. A., Rijnaarrts, H. H. M., Stams, F. J. M., de Kreuk, H. F., Schraa, G. & Bosma, T. N. P. (1998). Stimulation of Reductive Dechlorination for in situ Bioremediation of a Soil Contaminated with Chlorinated Ethenes. *Water Science and Technology*, 37(8), 105–110.
34. Mittal, K. L. (1979). Solution Chemistry of Surfactants. Plenum Press, New York.

35. Neville, C.J. (1990). Notes on properties of the unsaturated zone at CFB Borden. *Waterloo Centre for Groundwater Research.*
36. Prédélus, D. Lassabatere, L. Louis C. Gehan, H. Brichart, T. Winiarski, T. & Angulo-Jaramillo, R. (2017). Nanoparticle transport in water-unsaturated porous media: effects of solution ionic strength and flow rate. *Journal of Nanoparticle Research*, 19(3), 104.
37. Reddy, K. R., Semer, R., & Adams, J. A. (1999). Air flow optimization and surfactant enhancement to remediate toluene-contaminated saturated soils using air sparging, *Environmental Management and Health*, 10(1), 52-63.
38. Richert, S. H., Morr, C. V., & Cooney, C. M. (1974). Effect of Heat and Other Factors upon Foaming Properties of Whey Protein Concentrates. *Journal of Food Science*, 39, 42–48.
39. Rosen, M. J., & Kunjappu, J. T. (2012). Surfactants and interfacial phenomena. John Wiley & Sons.
40. Rothmel, R. K., Peters, R. W., St Martin, E., & Deflaun, M. F. (1998). Surfactant foam bioaugmentation technology for in situ treatment of TCE-DNAPLs. *Environmental Science & Technology*, 32(11), 1667–1675.
41. Schrick, B., Hydutsky, B. W., Blough, J. L., & Mallouk, T. E. (2004). Delivery Vehicles for Zerovalent Metal Nanoparticles in Soil and Groundwater. *Chemistry of Materials*, 16(11), 2187–2193. http://doi.org/10.1021/cm0218108
42. Shen, X., Zhao, L., Ding, Y., Liu, B., Zeng, H., Zhong, L., & Li, X. (2011). Foam, a promising vehicle to deliver nanoparticles for vadose zone remediation. *Journal of Hazardous Materials*, 186(2-3), 1773–1780. http://doi.org/10.1016/j.jhazmat.2010.12.071
43. Singh, R. & Misra, V. (2016). Stabilization of zero-valent iron nanoparticles: role of polymers and surfactants. *Handbook of nanoparticles*, 985-1007.
44. Song, B., Zeng, G., Gong, J., Liang, J., Xu, P., et al., (2017). Evaluation methods for assessing effectiveness of in situ remediation of soil and sediment contaminated with organic pollutants and heavy metals. *Environment International*, 105(January), pp.43–55. Available at: http://dx.doi.org/10.1016/j.envint.2017.05.001.
45. Srirattana, S. Piaowan, K. Lowry, G.V. & Phenrat, T. (2017). Electromagnetic induction of foam-based nanoscale zerovalent iron (NZVI) particles to thermally enhance non-aqueous phase liquid (NAPL) volatilization in unsaturated porous media: Proof of concept. *Chemosphere*, 183, pp.323–331. http://dx.doi.org/10.1016/j.chemosphere.2017.05.114.
46. Su, Y., Zhao, Y., Li, L.L., Qin, C., Wu, F., Geng, N.N. & Lei, G.S. (2014). Transport characteristics of nanoscale zero-valent iron carried by three different "vehicles" in porous media. 4529, pp.1639–1652.
47. Su, Y. Zhao, Y. Li, L. & Qin, C. (2015). Enhanced Delivery of Nanoscale Zero-Valent Iron in Porous Media by Sodium Dodecyl Sulfate Solution and Foam. *Environmental Engineering Science*. 32(8), pp.684–693.
48. Sun, Q. Li, Z. Li, S. Jiang, L. Wang, J. & Wang, P. (2014). Utilization of Surfactant-Stabilized Foam for Enhanced Oil Recovery by Adding Nanoparticles. *Energy & Fuels*, *28*(4), 2384-2394.
49. Stepan. (2012-2017). Chemical Manufacturing Company. http://www.stepan.com/default.aspx
50. Sigma-Aldrich. (2015-2016). Chemicals Company. https://www.sigmaaldrich.com/canada-english.html
51. Tratnyek, P.G. & Johnson, R.L., (2006). Nanotechnologies for environmental cleanup. *Nanotoday* 1(2), pp.44–48.
52. Theron, J., Walker, J.A. & Cloete, T.E., (2008). Nanotechnology and Water Treatment: Applications and Emerging Opportunities. *Critical Reviews in Microbiology*, 34, pp.43–69.

53. Urum, K., & Pekdemir, T. (2004). Evaluation of biosurfactants for crude oil contaminated soil washing. *Chemosphere*, 57, 1139–1150. http://doi.org/10.1016/j.chemosphere.2004.07.048
54. Urum, K., Pekdemir, T., Ross, D., & Grigson, S. (2005). Crude oil contaminated soil washing in air sparging assisted stirred tank reactor using biosurfactants. *Chemosphere*, 60, 334–343. http://doi.org/10.1016/j.chemosphere.2004.12.038
55. Wang, C. & Li, H.A. (2016). Stability and mobility of foam generated by gas-solvent/surfactant mixtures under reservoir conditions. *Journal of Natural Gas Science and Engineering*, 34, pp.366–375. Available at: http://dx.doi.org/10.1016/j.jngse.2016.06.064.
56. Wang, M. Gao, B. and Tang, D. (2016). Review of key factors controlling engineered nanoparticle transport in porous media', *Journal of Hazardous Materials*, 318, pp. 233–246.
57. Wang, H., & Chen, J. (2012). Enhanced flushing of polychlorinated biphenyls contaminated sands using surfactant foam: Effect of partition coefficient and sweep efficiency. *Journal of Environmental Sciences (China)*, 24(7), 1270–1277. http://doi.org/10.1016/S1001-0742(11)60881-4
58. Wang, S., & Mulligan, C.N. (2004a). An evaluation of surfactant foam technology in remediation of contaminated soil. Chemosphere, 57(9), pp.1079-1089.
59. Wang, S. & Mulligan, C. N. (2004b). Rhamnolipid Foam Enhanced Remediation of Cadmium and Nickel Contaminated soil. *Water, Air, and Soil Pollution*, 157, 315–330.
60. Yan, W. Lien, H. Koel, B.E. & Zhang, W. (2013). Iron nanoparticles for environmental clean-up: recent developments and future outlook. *Environmental Science: Processes & Impacts*, 15(1), 63-77.
61. Zhang, Z. F., Freedman, V. L., & Zhong, L. (2009). Foam Transport in Porous Media–A Review. Pacific Northwest National Laboratory: Washington.
62. Zhao, X., Liu, W., Cai, Z., Han, B., Qian T., & Zhao. D. 2016. An overview of preparation and applications of stabilized zero-valent iron nanoparticles for soil and groundwater remediation. *Water Research*, 100, pp.245–266. Available at: http://dx.doi.org/10.1016/j.watres.2016.05.019.
63. Zhong, L., Qafoku, N. P., Szecsody, J. E., Dresel, P. E., & Zhang, Z. F. (2009). Foam Delivery of Calcium Polysulfide to the Vadose Zone for Chromium(VI) Immobilization: A Laboratory Evaluation. *Vadose Zone Journal*, 8(4), 976–985. http://doi.org/10.2136/vzj2008.0124
64. Zhong, L., Szecsody, J. E., Zhang, F., & Mattigod, S. V. (2010). Foam Delivery of Amendments for Vadose Zone Remediation : Propagation Performance in Unsaturated Sediments. Vadose Zone Journal, 9, 757–767. http://doi.org/10.2136/vzj2010.0007
65. Zhong, L., Szecsody, J., Oostrom, M., Truex, M., Shen, X., & Li, X. (2011). Enhanced remedial amendment delivery to subsurface using shear thinning fluid and aqueous foam. *Journal of Hazardous Materials*, 191(1–3), 249–257. http://doi.org/10.1016/j.jhazmat.2011.04.074

Appendix A

Wang and Mulligan (2004a) performed a comprehensive evaluation of a number of laboratory and field studies that include surfactant foams to enhance soil remediation (Table A.1). All of these studies but the one conducted by Kommalapati et al. (1998) showed enhancement of the overall efficiency of organic compound removal. In all of these studies, foam was considered as a remediation reagent itself rather than a delivery vehicle. Moreover, in most of them, the experiments were conducted in a saturated medium. There exist only a few studies focusing on the use of foam as a delivery vehicle for remediation reagents (Shen et al. 2011; Zhong et al. 2011; Zhong et al. 2009; Rothmel et al. 1998).

Table A.1. Summary of studies on surfactant foam enhanced soil remediation [adapted from Wang and Mulligan, 2004a]

Description	Surfactant	Main results	Reference
Field demonstration of surfactant/foam process for aquifer NAPL (mixture of TCE, TCA, and PCE) remediation at Hill Air Force Base in Utah.	Sodium dihexylsulfosuccinate	The average DNAPL saturation of the swept volume was reduced to 0.03%	Hirasaki et al. (1997b)
Foam-enhanced surfactant solution flooding in removing *n*-pentadecane from contaminated column	Triton SP-series	Slightly over 74% of the *n*-pentadecane was removed at a gas-liquid ratio of 10/1	Huang and Chang (2000)
Micromodel study of surfactant foam remediation of residual TCE	Bioterge As-40	99% of the residual TCE was removed	Jeong et al. (2000)
Remediation of PAH-contaminated soils using foams	Biosurfactants + 50% ethanol	Foams readily desorbed PAHs from contaminated soils and moved well at pressure of 33.9 kPa/m (1.5 psi/ft) or less	Kilbane et al. (1997)
Soil flushing using colloid gas aphron (CGA) suspensions generated from a plant-based surfactant to remove HCB from soil	Natural surfactant from *Sapindus mukorossi* (Soapnut)	CGA suspension recovered 670 µg in 12 pore volumes compared to 8 µg by waterflood	Kommalapati et al. (1998)
Remediation with surfactant foam of PCP-contaminated soil	Triton X-100, JBR 425	Triton X-100 (1%) foam removed 85% and 84% of PCP from fine sand and sandy-silt, respectively	Mulligan and Eftekhari (2003)
Bench-scale study of surfactant foam/bioaugmentation technology for *in situ* treatment of TCE-DNAPLs	Steol CS-330	Injecting the foam in a pulsed operation removed 75% of the contaminant, and adding the microbes resulted in 95-99% degradation of the residual	Rothmel et al. (1998)

An example of the lab-scale studies is the work by Huang and Chang (2000) who investigated the efficiency of a foam flooding process for n-pentadecane removal. The authors compared surfactant solution and foam flushing processes in contaminated glass-bead columns and concluded that foam flushing gave better results in terms of the recovery of n-pentadecane compared with the results obtained from surfactant-solution flushing. Mulligan and Eftekhari (2003) used contaminated soil sediments and two surfactants (Triton X-100 and a commercial rhamnolipid, JBR 425) to generate foam, investigate its capability to remove pentachlorophenol (PCP) from the columns, and compare the results with those of surfactant solution injection. Based on the results, the Triton X-l00 foam (1%) removed more than twice as much PCP than the surfactant solution.

In another lab-scale study, Jeong et al. (2000) used a micromodel to assess residual trichloroethylene (TCE) removal by foam generated by an anionic surfactant, sodium C_{14-16} olefin sulfonate (Bio-terge AS-40). While the surfactant solution removed 41% of the residual TCE, surfactant foam removed 99%, using 25 pore volumes of the surfactant solution and the surfactant foam, respectively. Employing an anionic surfactant, sodium dodecyl sulfate (SDS), Couto et al. (2009) investigated the efficiencies of surfactant solution and foam for diesel oil removal from soil columns. Based on their results, the removal efficiency obtained by foams was more than that of solutions. Using lab-scale experiments, Wang and Chen (2012) assessed the removal efficiencies of polychlorinated biphenyl (PCB) from contaminated soil. Three surfactants, Triton X-100, SDS, and polyethylene glycol lauryl ether (Brij35), were used to prepare the solutions and foams. The authors used two types of quartz sand and concluded that foam was more effective in a porous medium with high porosity and low hydraulic conductivity. The authors also investigated an integrated water-solution-foam flushing approach that consisted of four steps: 5 pore volume water flushing, 10 pore volume surfactant solution flushing, 10 pore volume surfactant foam flushing, and 5 pore volume water flushing. They reported that PCB removal after the integrated approach was about 10% higher than that of surfactant foam flushing alone. Therefore, they concluded that the approach successfully incorporates the positive effects of the surfactant solution and foam flushing: the enhanced solubility and mobility control, respectively. Recently, two-dimensional sandbox tests were conducted by Longpr´e-Girard et al. (2016) to investigate the ability of surfactant foam to recover LNAPL in a saturated heterogeneous porous medium, consisting of two different types of silica sand with different grain sizes and permeabilities. Ammonyx Lo was the surfactant used in the tests, and p-xylene was used as the LNAPL. The results showed that after foam injection, only 0.29% of the initial mass of the LNAPL remained in the sandbox, which means nearly 100% p-xylene removal.

Using surfactant foams may lead to treatment cost reduction because of the low usage of surfactants compared with using solutions. Maire and Fatin-Rouge (2017) combined surfactant foam and surfactant solution flushing to investigate DNAPL removal in a shallow saturated contaminated soil at the bench-scale. They reported up to 60% of DNAPL removal by surfactant foam flushing with a low surfactant consumption (<0.4 $kgkg^{-1}$ DNAPL removed) using dihexylsulfosuccinate (DHSS) as the surfactant. Then, they combined the surfactant foam flushing with a surfactant solution flushing using the surfactant Tergitol 15S9, and they reported that the DNAPL removal was improved to ~95%. Based on the results, the surfactant consumption of the combined approach was 10 times lower than that of the surfactant solution flushing only. In another recent study, Maire et al. (2015) reported a 7.6 times lower usage of surfactant solution when the soil was flushed with foam to reach the similar removal amount as the surfactant solution flushing. The authors investigated DNAPL removal in a saturated contaminated soil at the bench-scale and reported that foam flushing in the column experiments resulted in higher DNAPL removal values compared to that of solution flushing only. In their contribution, Couto et al. (2009) reported that diesel oil removal from sandy soils obtained by surfactant solution and surfactant foam were 35% and 88%, respectively. They also concluded that the surfactant foams required a lower amount of surfactant compared to surfactant solutions.

Kilbane et al. (1997) investigated the efficiency of ethanol-based foams in the desorption of polyaromatic hydrocabons (PAHs) from weathered manufactured gas plant (MGP) site soils. By ethanol-based foams, the authors meant foams that were made by the solutions that, in turn, were made by dissolving the surfactants into a mixture of ethanol and water. Four surfactants (Triton X-100, Tween 80, Standapol ES-2, and IGT-FF52) were employed to generate aqueous and ethanol-based foams. The authors demonstrated that ethanol-based foams using the surfactant IGT-FF52 efficiently desorbed PAHs from MGP site soils and needed less pressure (~ 14 kPa or less) to move through soil comparing to the pressures required for aqueous foams (~83 to ~296 kPa). Another example of a study that used ethanol-based foams is the work by Chowdiah et al. (1998) who investigated the pressure gradients during foam flow through soils. One aqueous surfactant solution, using Standapol ES-2, and two ethanol-based surfactant solutions, using IGT-FF52 and IGT-FF13, were generated for foam flushing. Based on the Mulligan and Wang results, the pressure gradients of the flow of foams varied from about 905 kPa/m to 45 kPa/m for the aqueous foam and ethanol-based foams, respectively.

There are only a few studies that have focused on the use of foam as a vehicle for reagent delivery. Rothmel et al. (1998) investigated combining surfactant foam flushing with a bioaugmentation technology to remediate TCE DNAPLs. Three surfactants, Tergitol 15-S-12, Biosoft D-40, and Steol

CS-330 (sodium lauryl ether sulfate) were assessed, and strain ENV 435, the TCE-degrading bacteria, was used as the reagent. Based on the results, the foam generated by Steol CS-330 showed the highest efficiency for TCE mobilization. The authors also conducted further studies to assess a pulsed injection (foam/artificial groundwater/foam) and concluded that it was more successful in the mobilization and dispersion of TCE. Compared with the surfactant solution, surfactant foam led to improvement both in the dispersion and survival of the injected TCE-degrading bacteria. Delivering strain ENV 435, the TCE-degrading bacteria, with the second pulse of foam injection led to 95-99% degradation of the residual TCE. In another lab-scale study, Zhong et al. (2009) assessed the use of surfactant foam to deliver CPS into the unsaturated zone to immobilize chromium(VI). The surfactant Steol CS-330 was used to generate foam. The results indicated that the foam delivery of CPS can be successfully used to remediate the contaminated unsaturated zone. Shen et al. (2011) conducted column experiments using surfactant foam to deliver synthetic microspheres in unsaturated porous media. Foam was generated by sodium lauryl ether sulfate (SLES), and carboxyl-modified polystyrene microspheres were used as the substitute for nanoparticles. The authors also conducted preliminary experiments to evaluate the ability of foam to carry nano zero valent iron (nZVI) particles, and they concluded that the foam was capable of carrying notable fractions of nZVI particles. Zhong et al. (2011) conducted unsaturated column and cell experiments with foam delivery. They investigated the mitigation of technetium (Tc-99) mobilization by foam delivery of CPS into the columns and also explored foam delivery of a chemical and lateral delivery enhancement through the cell experiments in heterogeneously and uniformly packed systems, respectively. The surfactant Steol CS-330 with the concentration of 0.5% (w/w) was used in all the experiments, and phosphate was used as the chemical delivered by foam in the cell experiments. Based on the results, foam delivery of CPS led to immobilization of 68% of the Tc-99 in the contaminated sediment, whereas water delivery of CPS resulted in immobilization of only less than 9% of the total Tc-99. The authors also reported that foam led to a better result for phosphate distribution compared to that resulted from liquid injection in a heterogeneous system. Also, it was concluded that unlike liquid injection, foam injection resulted in an enhanced lateral delivery in a uniform porous medium.

Zhong et al. (2010) conducted a series of unsaturated column experiments to investigate a set of physical characteristics: foam front, liquid front and gas front, the effect of sediment permeability and foam quality on foam injection pressure, and pressure distribution and liquid uptake and distribution across the columns. The surfactant Steol CS-330 with the concentration of 0.5% (w/w) was used in all the experiments. Once the foam flowed through the column, the foam bubbles started rupturing, and no

foam front but the liquid front was observed at the beginning of the foam flow. Visual observation showed that the foam front started to appear after a certain time. By liquid uptake, the authors meant the amount of liquid that is sorbed to the sediment particles. Based on their results, the foam front had a retardation of 9.1 relative to the gas front, the pressure distribution was almost linear across the column, the effects of the foam injection rate and initial water content in the column on the liquid uptake distribution were inconsiderable in the region that was occupied by the foam, an increase in foam quality led to a decrease in foam injection pressure, and the effect of sediment permeability on the foam injection pressure depended on the foam injection rate. The authors claimed that foam retardation is a concern in an unsaturated medium, especially when foam is used as a delivery vehicle for gas.

There appears to be only one field-scale study on the application of a surfactant/foam process for organic compound removal. Hirasaki et al. (1997b) conducted the first field demonstration of a surfactant/foam process for DNAPL removal from a heterogeneous alluvial aquifer. The DNAPL at the site consisted of 70% TCE, 10% perchloroethylene (PCE), 10% 1,1,1-trichloroethane (TCA), and 10% other minor components. To form *in-situ* foam, in a period of 3.2 days, a solution that contained 3.5 wt% (active material) of the anionic surfactant sodium dihexyl sulfosuccinate was injected, and air injection was done at intervals of two hours at three injection wells on a rotating basis. The authors concluded that the process successfully reduced the average DNAPL saturation. The initial average DNAPL saturation was 0.3% (668 mg/kg) of the swept pore volume, which was reduced to 0.03% (77mg/kg soil) of the swept pore volume.

Foam Generation Methods

Different methods have been employed to generate foam, depending on the scale of the study, the type of experiments, and the mechanism of foam formation that is either pre-generation of foam or co-injection of solution and gas to generate *in situ* foam.

In their lab-scale study as a part of their experimental setup to generate foam, Maire and Fatin-Rouge (2017) used a syringe pump and a mass flow controller to inject surfactant solution and gas, respectively. They formed foam by co-injection of surfactant solution and gas into the soil column. In their 2D sandbox experiments, Longpr´e-Girard et al. (2016) used an acrylic column as the foam generation column, which was filled with glass beads, and each 2.5-centimeter glass bead layer in the column was separated with a stainless-steel screen. Before entering the foam generation column, air and surfactant solution passed through two valves that alternately opened at fixed time intervals and then, a “T” shaped tube caused them to mix. The foam generation column was directly connected to

the sandbox. Maire et al. (2015) used a short soil column (2 cm) to pre-generate foam before it entered 1- and 2-D soil cells. Surfactant solution and gas were passed concurrently through the short soil column. The solution was pumped with a syringe pump or a peristaltic pump, and a gas cylinder connected to a flow meter was used as the gas supply. Del Campo Estrada et al. (2015) used a piston pump and an El-Flow mass flow controller to inject surfactant solution and gas into the soil column, respectively. Two valves were used to control the injection of solution and gas, and no foam generation column was employed. Likewise, in their study of surfactant foam, Wang and Chen (2013, 2012) generated foam without using a foam generation column. Foam was generated by concurrently injecting gas and surfactant solution through a "T" shaped metal mixer and a porous material. Before being injected into the metal mixer, the rates of solution and gas flow were controlled by flow meters.

Zhong et al. (2011) used the same foam generation setup as it was used by Zhong et al. (2010) and Zhong et al. (2009). The authors employed a glass column as the foam generation column, and a porous plate was installed at the bottom of the column for flow distribution. A liquid chromatography pump was used to pump the solution, and a gas flow controller was used to control the gas flow rate. The solution and gas flows were combined and led to the foam generation column. In their study, Shen et al. (2011) used a foam generation setup similar to what was used by Zhong et al. (2011). A plexiglass column was employed as the foam generation column, and three stainless wire screens were positioned at both the inlet and outlet of the column. Gas and solution were introduced into the column by passing through a three-way valve. Before entering the three-way valve, the gas flow rate was controlled and then, measured by a flow meter, and solution was pumped by a peristaltic pump. The gas and solution flow rates were modified such that the liquid level in the column was constant, and the foam bubbles were uninterruptedly generated.

In a study of remediation of sandy soils, Couto et al. (2009) employed a glass column with a porous disc installed at the bottom of it to generate foam. Foam was generated uninterruptedly by introducing air and surfactant solution to the bottom of the foam generation column such that there was a layer of surfactant solution on the porous disc during the foam generation. Surfactant solution was pumped using a peristaltic pump, and both solution and air flow rates were measured by rotameters. In a study of remediation of heavy metal-contaminated soil by Mulligan and Wang (2006), the authors used the same experimental setup for foam generation as it was used by Wang and Mulligan (2004b). A plastic column with porous stone plates was employed as the foam generation column. Air and surfactant solution were introduced to the column to generate foam. A pump was used to pump surfactant solution,

and two flow meters were employed to measure the flow rates of air and solution before entering the column. Surfactant solution and air flow rates could be varied separately to control the foam quality and flow rate. Oliveira et al. (2004) used a glass column to generate foam in their study on the effect of hydrophobic fine particles on the surfactant foam stability and foaming ability. A porous disc was installed at the bottom of the column, and air was flushed to the column through the porous disc, and the air flow rate was measured by a flow meter before entering the column. The surfactant solution was poured from the top of the column and then, foam generated.

In their micromodel studies, Jeong and Corapcioglu (2003a & 2003b) used an injection tube connected to the micromodel. Foam was generated in the injection tube by concurrently injecting air and surfactant solution. Mulligan and Eftekhari (2003) used a column at the top of which a porous stone was installed. Surfactant solution and air were injected through the porous stone to generate foam. Surfactant solution was pumped, and the rates of surfactant solution and air were measured by two flow meters before being injected into the foam generation column. Huang and Chang (2000) used a chamber that consisted of a drawn tip. The chamber was filled with surfactant solution, and the drawn tip extended into the chamber. To generate foam, nitrogen was passed through the tip, and surfactant solution was injected into the chamber from the other end of the chamber. A peristaltic pump was used to pump the surfactant solution to the chamber, and a flow meter was used to measure the rate of nitrogen flow before it entered the chamber. In a micromodel study, Jeong et al. (2000) used a "T" shaped tube connector as a foam generator. Surfactant solution and air were injected into the "T" shaped tube using two syringe pumps. Consequently, a surfactant-alternating-gas foam was generated and then, injected into the micromodel. Ripley et al. (2000) used a column packed with glass beads to generate foam. Foaming agent solution and gas were mixed in the column and then, foam was generated and passed through a nozzle that was connected at the end of the foam generation column. In their study on the foam flow behavior in porous media, Zhong et al. (1999) generated foam by alternately injecting surfactant solution and air into a core packed with glass beads. Chowdiah et al. (1998) used a porous disc to generate foam. The authors generated foam by simultaneously injecting surfactant solution and air into the porous disc. To control the foam quality and foam flow rate, air and surfactant solution injection rates could be varied separately. In their lab-scale studies, Hirasaki et al. (1997a) injected surfactant slugs alternating with gas injection to generate foam. A syringe pump was used to inject surfactant solutions, and to inject gas, either a mass flow controller, a syringe pump, or a pressure regulator was employed. Also, in their field demonstration, Hirasaki et al. (1997b) generated foam *in situ* by injection of gas intermittently but concurrently with surfactant solution such that the surfactant

solution always flowed through the injection well, and the gas was injected into the injection well on a rotary basis and with a two-hour period of injection per well. Llave and Olsen (1994) used a fired Berea core as a foam generator. Gas and surfactant solution were concurrently injected into the foam generator and then, foam was generated. To provide visual observation of foam before it was injected into the primary soil core, a sight glass was used in-line between the foam generator and the soil core.

Appendix B

Table B.1. The sets of weights for criterion weight uncertainty

Criterion	Surfactant Type	Health Hazard	Biodegradability	Charge Type	CMC	Cost
Weight Set 1	0.0400	0.0800	0.0800	0.1600	0.4000	0.2400
Weight Set 2	0.0800	0.0400	0.0800	0.1600	0.4000	0.2400
Weight Set 3	0.0800	0.0800	0.0400	0.1600	0.4000	0.2400
Weight Set 4	0.0833	0.0417	0.0417	0.1667	0.4167	0.2500
Weight Set 5	0.0417	0.0833	0.0417	0.1667	0.4167	0.2500
Weight Set 6	0.0417	0.0417	0.0833	0.1667	0.4167	0.2500
Weight Set 7	0.0769	0.0769	0.0769	0.1538	0.3846	0.2308
Weight Set 8	0.0851	0.0213	0.0426	0.1702	0.4255	0.2553
Weight Set 9	0.0851	0.0426	0.0213	0.1702	0.4255	0.2553
Weight Set 10	0.0426	0.0851	0.0213	0.1702	0.4255	0.2553
Weight Set 11	0.0213	0.0851	0.0426	0.1702	0.4255	0.2553
Weight Set 12	0.0426	0.0213	0.0851	0.1702	0.4255	0.2553
Weight Set 13	0.0213	0.0426	0.0851	0.1702	0.4255	0.2553

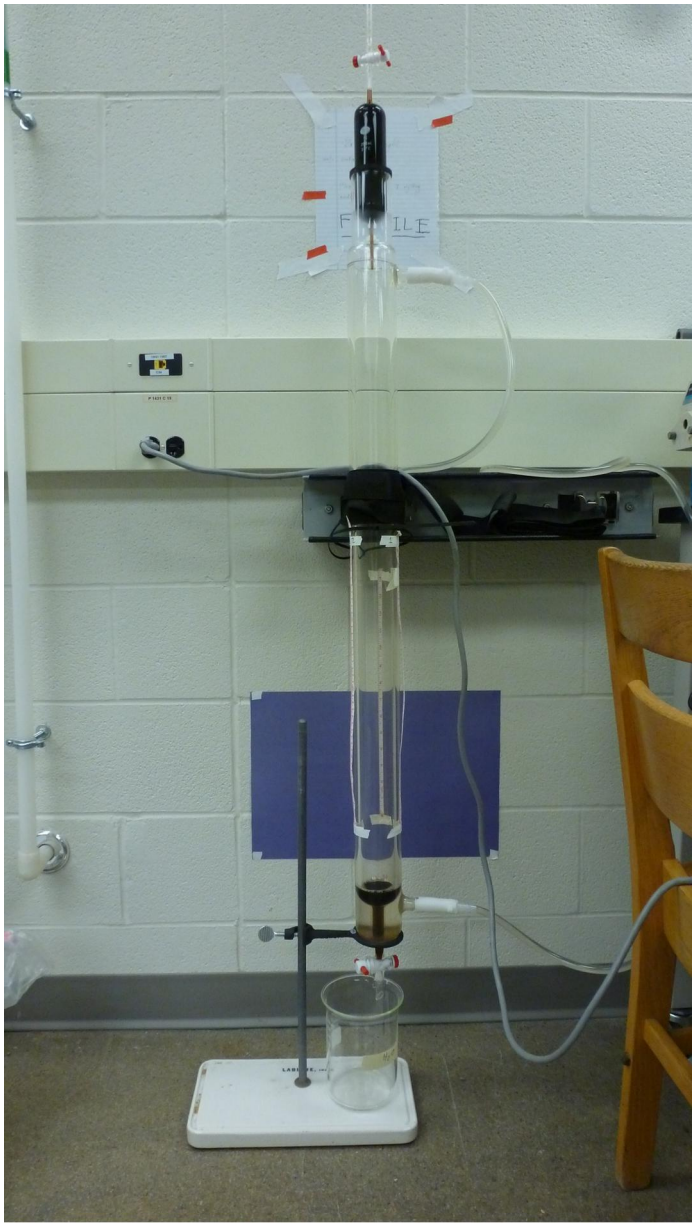

Figure B.1. The Ross Miles test apparatus